THE PEOPLE'S DEMOCRATIC REPUBLIC OF ALGERIA

MINISTRY OF HIGHER EDUCATION AND SCIENTIFIC RESEARCH

ECHAHID HAMMA LAKHDAR UNIVERSITY - EL OUED

FACULTY OF SCIENCE AND TECHNOLOGY

Department of Electrical Engineering

End of studies thesis presented to obtain the diploma of

ACADEMIC Master

Domaine : *Science et Technologie*

Filière : *Electrotechnique*
Option: *Electrical Control*
Presented by :

Abdelkarim Dou

Study and Realization of a Photovoltaic System With an MPPT Control

In front of the jury composed of:

Dr.Mammeri Ossama	***President***	***Univ. Eloued***
Dr.Labbi Yacin	***Superviso***	***Univ. Eloued***
Dr.Gacem Abdelmalek	***Examiner***	***Univ. Eloued***

2021/2022

Dedication

To our dear parents, for the great love with which they have surrounded us since our birth, for their patience, their sacrifices and their encouragement.

To our dear brother and sisters wishing them success in their lives.

To all our friends from Echahid Hamma Lakhdar University of El-oued and elsewhere for the pleasant moments we spent together .

To all those who helped us during our training to all of them we dedicate this modest work.

Thanks

First and foremost, we would like to thank Almighty God for granting us the strength and courage to complete this work.

We would like to express our sincere thanks to our supervisor for the theme Dr. LABII YACIN.

We kindly ask you to accept the testimony of our deepest gratitude and our deep respect.

We also present our sincere thanks to the entire teaching team of the electrical engineering department of Echahid Hamma Lakhdar University. el-oued.

Special for Dr. Gacem Abdelmalek for his orientation his daily availability his numerous advice and for his encouragement , Mr.OBEIDI NABIL for his helping during the demo part of this letter and Dr.LABIED CHOUAIB for his assistance scientific, human quality , importance and support for our work .

We particularly thank our families for their moral support for this work, thank you for encouraging us, and believing in us.

We also thank our friends, our classmates, who encouraged us throughout this project and helped us a lot.

index of symbols

E: Lighting (W/m2).

I_{ph}: The photo-current (A).

I: The current generated by the solar cell (A).

I_s: The saturation current (A).

I_{sc}: the short-circuit current (A).

IL: The chopper inductance current (A).

I_{pv}: Current delivered by the PV generator (A).

V: the voltage across the cell (V).

q: The charge of the electron =1.6.10-19 C.

·Rs: The series resistance (Ω).

Rsh: The Shunt Resistor (Ω).

T: The operating temperature in Kelvin.

A: the quality factor of the cell.

Vth: The thermal voltage.

Voc: The open circuit voltage (V).

P: The characteristic power (W).

Pmax: The maximum power (W).

FF: Form factor.

Ns: Number of modules in the panel in series.

Np: Number of modules in the panel in parallel.

V_{opt}: Optimal voltage (V).

I_{opt}: Optimum current (A).

G: Reference illumination (1000 W/m2).

C: Chopper output filter capacitor [μF].

L: Chopper inductance.

Q: The chopper switch.

CS: Static Converter.

D: Duty cycle..

Abbreviation used

PV: Photovoltaic.

GPV: Photovoltaic Generator.

MPPT: Maximum Power Point Tracking.

P&O: Disturbance and Observation.

DC: Direct Current

DC-DC: DC-DC conversion

PSO: Particle swarm optimization

Inc.CoN: Increment of conductance

الملخص:

تكتسب الطاقة الكهروضوئية(PV) ماكانتها بشكل متزايد في مصادر الطاقة البديلة، لكن الالواح الشمسية، على الرغم من التطور في تقنيات التصنيع، تعاني من كفاءة تحويل طاقة منخفضة إلى حد ما، ويمكن أن تكون هذه الكفاءة أقل اذا لم يعمل المولد الكهروضوئي (PVG) حول نقطة تسمى: نقطة الطاقة القصوى MPP .يعد السعي وراء هذه النقطة، التي تغير الموقع مع الظروف المناخية، خطوة مهمة للغاية في تشغيل نظام الكهروضوئية. سنقوم في هذه الأطروحة بمحاكاة وتحسين وتحقيق نظام كهروضوئي يعمل مبحول DC-DCالخافض والرافع لجهد. تغطي هذه الدراسة تنفيذ خوارزميات مختلفة لأقصى نقطة للطاقة مثل خوارزمية الاضطراب والمراقبة (O&P)، والتوصيل الاضافي (InC)، Cuckoo search (CS) ذلك سنبدأ بمحاكاة ونمذجة الخلية الضوئية ومحولDC-DC الخافض والرافع لجهد وفقًا للمنوذج الرياضي، بعد ذلك، قمنا بتفصيل العديد من خوارزميات MPPT التي تتحكم في المحول الخاص بنا. أخير، حققنا التطبيق العملي لنظامنا مع الخوارزميات الثلاثة المقترحة MPPT استنادا الى لوحة Arduino Mega 2560 .

الكلمات المفتاحية: مولد الطاقة الكهروضوئية، ، P&O، INC، CS، 2560 Arduino Mega،MPPT.

Abstract:

Photovoltaic (PV) energy is increasingly gaining its place in alternative energy sources, but solar panels, despite the development in manufacturing techniques, suffer from a rather low energy conversion efficiency, and this efficiency can be lower if the photovoltaic generator (PVG) is not working. Around a point called: the maximum power point MPP. The pursuit of this point, which changes location with climatic conditions, is a very important step in the operation of the PV system. In this thesis, we will simulate, improve and realize a DC-DC step-down and step-up photovoltaic system. This study covers the implementation of various max power point algorithms such as perturbation and control (O&P) algorithm, additional conduction (InC), Cuckoo search (CS) that we will start by simulating and modeling the photovoltaic and DC-DC step-down transformer according to the mathematical model, after that, we detail several MPPT algorithms that control our converter. Finally, we have achieved the practical application of our system with the three proposed MPPT algorithms based on the 2560 Arduino Mega board.

Résumé:

L'énergie photovoltaïque (PV) gagne de plus en plus sa place dans les sources d'énergie alternatives, mais les panneaux solaires, malgré l'évolution des techniques de fabrication, souffrent d'un rendement de conversion d'énergie assez faible, et ce rendement peut être plus faible si le générateur photovoltaïque (PVG) n'est pas Autour d'un point appelé : le point de puissance maximale MPP La poursuite de ce point, qui change de localisation avec les conditions climatiques, est une étape très importante dans le fonctionnement du système PV. Dans cette thèse, nous allons simuler, améliorer et réaliser un système photovoltaïque DC-DC abaisseur et élévateur. Cette étude couvre la mise en œuvre de divers algorithmes de point de puissance maximale tels que l'algorithme de perturbation et de contrôle (O&P), la conduction supplémentaire (InC), la recherche de coucou (CS) que nous commencerons par simuler et modéliser le transformateur abaisseur photovoltaïque et DC-DC selon le modèle mathématique, après cela, nous détaillons plusieurs algorithmes MPPT qui contrôlent notre convertisseur. Enfin, nous avons réalisé l'application pratique de notre système avec les trois algorithmes MPPT proposés basés sur la carte Arduino Mega 2560.

TABLE of contents

Dedication .....

Thanks .....

List of symbols .....

Abstract: .....

TABLE of contents .....

Table Figue .....

Table index **14**

INTRODUCTION **15**

CHAPTER I: .....

GENERAL INFORMATION ON SOLAR ENERGY **17**

I.1. Introduction : *2*

I.2. Solar energy: *3*

I.3. Assessment of renewable energy in Algeria: *3*

I.4. Solar Energy and the Photovoltaic Effect: *4*

I.4.1. Principle of the Photovoltaic Effect: 4

I.4.2. Solar Cell and Modeling 5

I.4.3. External parameters of a photovoltaic cell: 9

I.5. Photovoltaic module: *11*

I.5.1. Grouping of photovoltaic cells in parallel: 12

I.5.2. Grouping of photovoltaic cells in series: 13

I.6. Effects of Climatic Variations on the Photovoltaic module: *14*

I.6.1. Influence of illumination: 14

I.6.2. Influence of temperature 15

I.7. Applications of photovoltaic energy: *15*

I.7.1. Standalone apps: 15

I.7.2. Non-standalone applications: 16

I.8. Direct connection (load source): *17*

I.9. Advantages and disadvantages of a PV installation: *18*

a) Advantages 18

b) Disadvantages 18

I.10. Conclusion *19*

CHAPTER II **2**

STUDY OF DC/DC CONVERTERS **2**

II-1. Introduction *21*
II.2. DC/DC converters 21
II.2.1.1. Composition of the converter 23
I1.2.2 Boost Chopper (Boost) 26
II.2.3Buck-Boost chopper 27
II.3. Principle of operation of the DC-DC converter for the MPPT tracking *28*
II.3.1. Hacheur série ou abaisseur (Buck). 29
II.3.2. Parallel Chopper or Booster (Boost) 29
II.3.3. Series-Parallel or Buck-Boost chopper 30
II.4. Buck-Boost Converter Analysis *31*
II.4.1. Functioning 31
II.4.2. Calculation of Buck-Boost quantities 32
II.4.3. Sizing of the Buck-Boost converter 34
II.5. Conclusion *36*
CHAPTER III 37
MPPT Methods 37
III.1. Introduction *38*
III.2. Need for maximum power point tracker *38*
III.3 .The maximum power point tracking process *39*
III. 4. Hill-climbing techniques *40*
III.4.1 Perturb and observe 40
III.4.2 Incremental conductance (IC) method 42
III.5. Fuzzy logic control: *46*
III.6. Neural networks: *48*
VI.1. Introduction *51*
VI.2. Simulation of a photovoltaic system *51*
VI.2.1 Matlab/Simulink diagram of photovoltaic system 52
VI.2.2 Simulation results: 54
e) Simulation results of MPP tracking waveforms *58*
FigureVI. : *Simulation results of MPP tracking waveforms: (A) duty cycle, (B) PV power, (C) PV current and (D) PV voltage for steady state operation with two setting factors MPPT scale: (blue) PO based on 0.01 and (red) PO based on 0.0025.* *58*
VI.3. Material used *58*
VI.3.1 The microcontroller 58

VI.3.2 The solar panel 60
VI.3.3 Buck-Boost Converter 61
VI.4. Realization of the system *62*
VI.4.1 Practical results 64
VI.5.Conclusion *67*
CONCLUTION **68**
BIBLIOGRAPHIE **70**

Index of picter

Figue I.1: Evolution of world electricity consumption (Mtoe). 2

Figue I.2 : Distribution of uses of the RE sector in Algeria 3

Figue I.3: Cross section of a typical PV cell 5

Figue I.4: Schéma équivalent d'une cellule solaire 6

Figue I. 5: : Simplified equivalent diagram of a real solar cell connected to a load. 7

Figue I.6: Characteristic $I_{cell} = f(V_{cell})$ of a photovoltaic cell 8

Figue I. 7 : a cell, a module and a photovoltaic panel 11

Figue I. 8: Characteristic I= f(V) of a photovoltaic module and operating zones 11

Figue I.9 : Characteristic of number of modules in parallel 12

Figue I.10 : Characteristic of number of modules in series conclusion 13

Figue I.11: The influence of illumination on P=f(V), et I=f(V) 14

Figue I.12 : The influence of temperature on the characteristics P=f(V), et I=f(V) 15

Figue I.13 : Example of the structure of a stand-alone PV system 16

Figue I.14: Example of the structure of a PV system connected to the network 16

Figue I.15 : Direct source-load connection 17

Figue I.16 : GPV operating points in direct connection to the load. 17

Figue II.1. Real buck converter. 22

Figue II.2. Circuit buck converter topologies. 22

Figue II.1. Symbolic representation and notation for the N-channel MOSFET. 23

Figue II.2. Structure of a low-power MOSFET cell 24

Figue II.3. single inductor L. 25

Figue II.4. Real Booster Converter. 26

Figue II.5. Circuits of the boost converter topologies. 26

Figue II.6. Real buck-boost converter. 27

Figue II.7. Circuits of Buck-Boost converter topologies. 28

Figue. II.8. Block diagram of a step-down chopper (Buck) 29

Figue. II.9. Block diagram of a step-up chopper (Boost) 30

Fig. II.10. Block diagram of a step-down chopper (Buck-Boost) 30

Figue. II.11. Buck-Boost Chopper Waveforms 31

Figue. II.12. The shape of the current flowing through the input capacitor 33

Figue III. 1: Block diagram of a typical MPPT system. 39
Figue III. 2: Solar array characteristic curves. 40
Figue III. 3: PV panel characteristic curves. 41
Figue III. 4: Flowchart of perturb and observe algorithm. 41
Figue III. 5: Flowchart of incremental conductance algorithm. 42
Figue III. 6: P-V curve depending on the irradiation. 43
Figue III. 7: Membership functions. 46
Table III: Rules Base table. 47
Figue III.8: Flowchart of the fuzzy logic control. 48
Figue III. 9: Neural network. 48
Figue VI.1: Data on the electrical characteristics of the PV module taken from Mat- ... 51
Figue VI.2 : Matlab/Simulink diagram of PV system with stable radiation. 52
Figue VI .3 : Matlab/Simulink diagram of PV system with variable radiation. 53
Figue VI.4 : Matlab/Simulink diagram of PV system (CS). 53
Figue VI.5 : Power PV simulation result 54
Figue VI.6 : PV voltage simulation result 54
Figue VI.7 : Changement de rapport ciclique à l'aide 55
l'algorithme suivi par le carte d'arduino. 55
Figue VI .8 : Power PV simulation result 55
Figue VI.9 : PV voltage simulation result**.** 56
Figue VI .10: Cyclic gear change using 56
the algorithm followed by the arduino board. 56
Figue **VI**.11 : Power PV simulation result 57
Figue VI.12: Cyclic gear change using 57
the algorithm followed by the arduino board. 57
Figue VI .13 : Arduino MEGA2560. 59
Figue VI .14 : Photo real PV panel. 60
Figue VI.16: Real photo of Buck-Boost converter board. 61
Figue VI.17: Real photo of Buck-Boost converter 62
Figue **VI**.18 : Real photo of control part of our system 63

Figue **VI**.19 :Real photo of PV system. 63

Figue VI.20: Practical result of the PO algorithm. 64

Figue VI.21 : Practical result of the INC algorithm 64

Figue VI.22: Practical result of the PO algorithm. 65

Figue VI.23 :Practical result of the INC algorithm. 65

Figue VI.24 : Practical result of the INC algorithm. 66

F**igue VI**.25: PWM signal 66

Figue VI.26 : Output voltage change by PWM constant control [0.9;0.1]. 67

Table index

TableI.1 : Solar potential in Algeria.....4
Table II. Electrical characteristics of the SLK60P6 panel from Siliken. 34
Table VI.1 : Buck-Boost converter parameter. 52
Table VI.2 : the arduino MEGA board**.** 59

INTRODUCTION

ITRODUCTION

Energy production is a challenge of great importance for the years to come. Indeed, the energy needs of industrialized societies are constantly increasing. Furthermore, developing countries will need more and more energy to carry out their development. Today, a large part of the world's energy production comes from fossil sources. The consumption of these sources results in greenhouse gas emissions and therefore an increase in pollution. The additional danger is that excessive consumption of the stock of natural resources reduces the reserves of this type of energy in a dangerous way for future generations.

By renewable energy, we mean energy from the sun, wind, heat from the earth, water or even biomass. Unlike fossil fuels, renewable energies are energies with unlimited resources. Renewable energies include a number of technological sectors depending on the source of energy used and the useful energy obtained. The direct exploitation of solar energy by means of sensors involves two very distinct technologies: one produces calories, it is solar thermal energy, and the other produces electricity .

In this thesis, we are mainly interested in the development of an optimization procedure which allows the point tracking of the maximum power (Maximum Power Point Tracking MPPT) of a photovoltaic generator (GPV), for a good exploitation of the generator. photovoltaic. This requires the implementation of a maximum power point tracking technique, such as the Perturbation-Observation (P&O) method and the Fuzzy approach. Thus, we present in this project the simulation under matlab/simulink and the realization of a digital MPPT control based on two MPPT algorithms which are P&O, INC, by making a realization by means of 'an Arduino Mega 2560 board with an MPPT control.

The thesis consists of three chapters:

In the first chapter we will present a generality on photovoltaic systems. By presenting the photovoltaic generator and the principle of photovoltaic conversion, then the modeling of the photovoltaic module.

In the second chapter, we studied DC-DC converter commonly used in photovoltaic systems (the bak Boost converter) then we studied modeling and the operating principle.

The third chapter is devoted to the principle of search in PPM, we have introduced many mppt algorithms and explained the principle of each of them and In the last chapter we will present the results of simulation and experimental tests

Finally, we will end our thesis with a general conclusion that will summarize the interest of our study

CHAPTER I:

GENERAL INFORMATION ON SOLAR ENERGY

I.1. Introduction :

The different sources of energy available in the world, apart from nuclear and geothermal energies, are all of solar origin. Indeed, even coal and oil come from plants, which depend on the sun. Nature transforms solar energy into many other sources, but never into electricity. To reach this stage, man is obliged to apply additional transformations to these sources which will reduce the overall efficiency of energy conversion. In what follows, we will first focus on the different existing energy sources in the world, specifying photovoltaics as a method of direct conversion of solar photons into electricity.

During the last decades, the world consumption of energy has considerably increased, this increase is due to the increase of the world population on the one hand and the explosion of the industrial development of the industrialized countries.

Currently the production of energy is based on non-renewable energies, namely petroleum, natural gas, coal and uranium (Figue I.1) [1].

Following the increase in the rate of world consumption of energy, the more the two serious problems posed by these energies: on the ecological level (pollution and global warming) and on the political between countries (conflicts between states to control fossil fuel reserves), these sources are exhaustible. Thus man will be condemned to find other sources to satisfy the energy needs of future generations. Energies say renewables are the best solution to overcome these problems. The production of these energies are based on forces or resources whose stocks are unlimited.

Figue I.1: Evolution of world electricity consumption (Mtoe).

There are several types of renewable energies, namely: geothermal energy comes from the heat of the depths of the earth. Hydroelectric energy, wind energy, biomass energy and solar energy. These types of energy come directly or indirectly from the sun [1].

I.2. Solar energy:

The sun is an almost inexhaustible source of energy that sends radiation to the surface of the earth which represents approximately 8400 times the energy consumption of humanity each year. This corresponds to an instantaneous power received of 1kWp/m2 distributed over the entire spectrum, from ultraviolet to infrared. The deserts of our planet receive in 6 hours more energy from the sun than humanity consumes in a year.

Solar energy is produced and used by several processes:

- **Thermal solar energy:** which simply consists of producing heat using dark panels. You can also produce with steam from the heat of the sun and then convert the steam into electricity.
- Photovoltaic solar energy: which consists of producing electricity directly from light using solar panels. This form of energy is already exploited in many countries, especially in countries or regions that do not have conventional energy resources such as hydrocarbons or coal.
- **Passive solar energy:** is another form of using solar energy which consists of using light directly for heating [2].

I.3. Assessment of renewable energy in Algeria:

The renewable energy potential in Algeria is the largest in North Africa. The market for renewable energies is promising and their promotion is one of the axes of the country's energy and environmental policy. Among the objectives announced by the public authorities, the local market must reach 500 MW this year 2010, bringing the share of electricity produced by renewable energies to 5% of the total electricity produced[3].

The breakdown of installed power by application:

Application	Powerful installed (Kw)	Percentage %
Electrification	1353	58 %
Télécommunication	498	21 %
Pumping	288	12 %
Public lighting	48	2 %
Autres	166	7 %

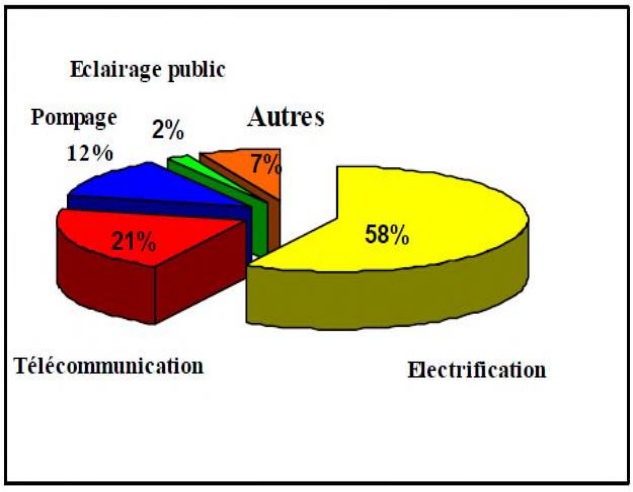

Figue I.2 : Distribution of uses of the RE sector in Algeria

- Solar potential:

Due to its privileged location, Algeria has the largest solar resource in the Mediterranean basin. The average sunshine duration of the Algerian territory exceeds 2000 hours per year, to reach nearly 3500 hours of sunshine in the Sahara desert. The total energy received is estimated at 169,400 TWh/year, i.e. 5,000 times the consumption

of annual electricity in the country The following table shows the rate of sunshine in Algeria [4]Regions	**Coastal regions**	**Highlands**	**Sahara**
Average duration	2650	3000	3500
Average energy received (KWh/m²/an)	1700	1900	2650

Table I.1 : Solar potential in Algeria

I.4. Solar Energy and the Photovoltaic Effect:

Electricity is one of the most versatile forms of energy and one that best adapts to every need. Its use is so widespread that today one could hardly conceive of a technically advanced society that does not use it. Thousands of devices are designed to operate using electrical energy, either in the form of low voltage direct current or from higher voltage alternating current. It is very interesting to produce electricity with a safe and non-polluting source of energy. There are two methods to be able to convert solar energy into electricity, depending on whether kinetic energy is used as an intermediate form of the process of conversion:

- Thermodynamic conversion systems.
- Direct systems, based on the physical interactions between the photons of the incident radiation and the electrons of the material, the photovoltaic effect, such as solar energy.

I.4.1. Principle of the Photovoltaic Effect:

It is the conversion of the energy carried by photons of light when they collide with suitably treated semiconductor materials, into electrical energy capable of creating a current of electrons through an external circuit. The key for produce a useful electric current is to be able to extract the released electrons.

One way to do this is to introduce chemical elements into the semiconductor material that help produce an excess of electrons and holes. These elements, which significantly alter the intrinsic properties of the semiconductor, are called dopants and the material is said to be doped when the process of incorporation into the semiconductor is complete.

A suitable dopant for silicon is boron. The structure created is called a P-type (positive) semiconductor. Another possible dopant for silicon is phosphorus. The semiconductor is said to be of type N (negative). If photons of incident light impart energy to electrons in the semiconductor, some electrons may cross the potential barrier, being expelled out of the semiconductor in a circuit.

outside. This generates an electric current. The electrons, after having traversed the external circuit, return in the semiconductor by the opposite face.

The semi-conductor material therefore does not store electrical energy but generates it by transforming the incident energy. Quantum physics predicts a theoretical efficiency for the silicon cell of 26% but the commercial cells obtained industrially do not rise above 17%. These values, implying a limitation on the electrical power that can be obtained, show that only a small part of solar energy can generate electricity.

I.4.2. Solar Cell and Modeling

Figue (I.3) shows the cross section of a typical PV cell:

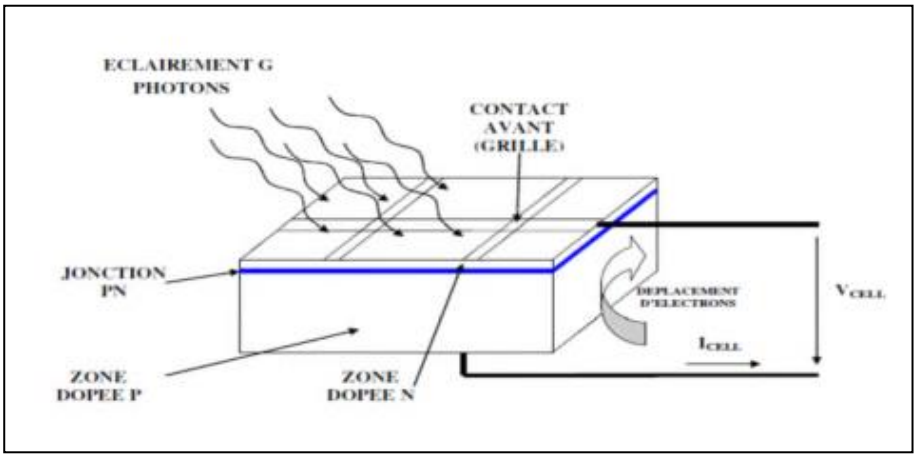

Figue I.3: Cross section of a typical PV cell

The photovoltaic cell is made of a P-N type semiconductor material.

The size of each cell ranges from a few square centimeters up to 100 cm2 or more. Its shape is circular, square or derived from both geometries.

The maximum cell voltage is about 0.6V for zero current. This voltage is called open circuit voltage Voc. The maximum current occurs when the cell terminals are short-circuited, it is called short-circuit current (Isc) and strongly depends on the level of illumination. A PV cell has, as we see in Fig. (I.4), a nonlinear I=f(V) characteristic with a PPM.

A real solar cell can be modeled by the electrical diagram below:

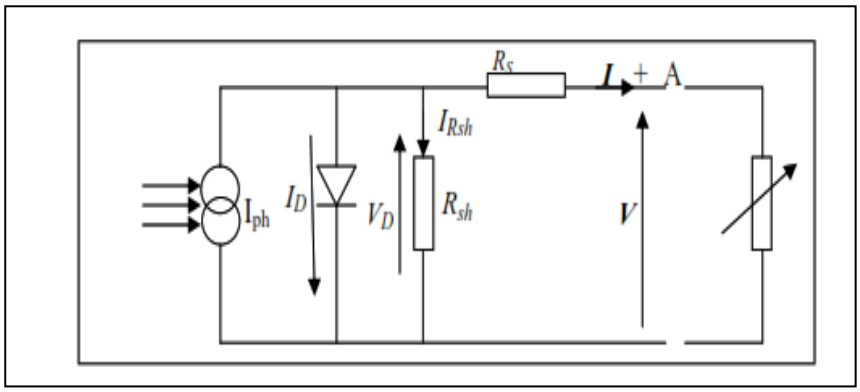

Figue I.4: Schéma équivalent d'une cellule solaire

Thus, a PV cell consisting of a silicon-based PN junction can be modeled by the following equation:

$I=I_{ph} – I_D - I_{sh}$……..……..……(I.1)

$$I = I_{ph} - \left[exp\left(q\frac{v+R_SI}{AKT}\right) - 1\right] - \frac{v+R_sI}{R_{sh}} \quad \text{…….……(I.2)}$$

$$V_{th=}\frac{AKT}{q} \quad \text{……..……..……..……..} \quad \text{(I.3)}$$

I_{ph}: The current photo.

I: The current generated by the solar cell.

V: the voltage across the cell.

R_S: The series resistance.

R_{Sh}: The shunt resistor.

I_s: the saturation current.

q: the charge of the electron =1.6.10-19 C.

A: the quality factor of the cell.

K: Boltzmann's constant = 1.38. 10-23 D/K.

T: the operating temperature in Kelvin.

V_{th}: The thermal voltage (a temperature dependent parameter).

Five parameters must be evaluated, whatever the conditions of illumination and temperature, these are R_S, I_s, I_{ph}, R_{Sh}, V_{th}

They can be determined as follows:

- V_{oc}: the open circuit voltage.
- I_{sc} : the short-circuit current.
- P : the characteristic power.
- Pmax: the maximum power .
- the form factor FF, and the efficiency.Des brèves définitions de ces paramètres, ainsi que their determinations of the characteristic are given below [1].

The quality factor of cell A depends on the recombination mechanisms; it is equal to 2 for crystalline cells and between 1 and 2 for amorphous cells. It is close to 1 for high currents and increases to 2 for low currents [4].

The resistance comes from the losses by recombinations due essentially to the thickness, to the effects of surface, as well as to the non-ideality of the junction. In practice this resistance is very large compared to the series resistance (the order of mega Ohms), its effect is neglected.

This results in a simplified equivalent electrical circuit as shown in the Figue below:

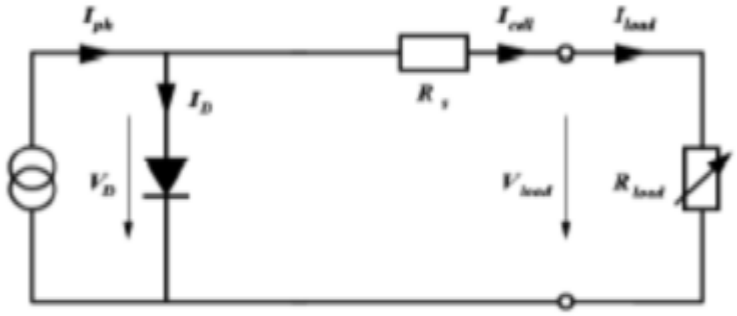

Figue I. 5: : Simplified equivalent diagram of a real solar cell connected to a load.

And its original equation (1.2) then becomes

$$I = I_{ph} - I_s \left[exp\left(q \frac{V+R_S I}{AKT} \right) - 1 \right] \text{ ……. ……..….(I.4)}$$

A PV cell has as we see in Figue (6), a characteristic

I = f(V) et P= f(V) non-linear . The use of the electrical model of the PV cell allows to simulate its behavior in the MATLAB environment of Mathworks.

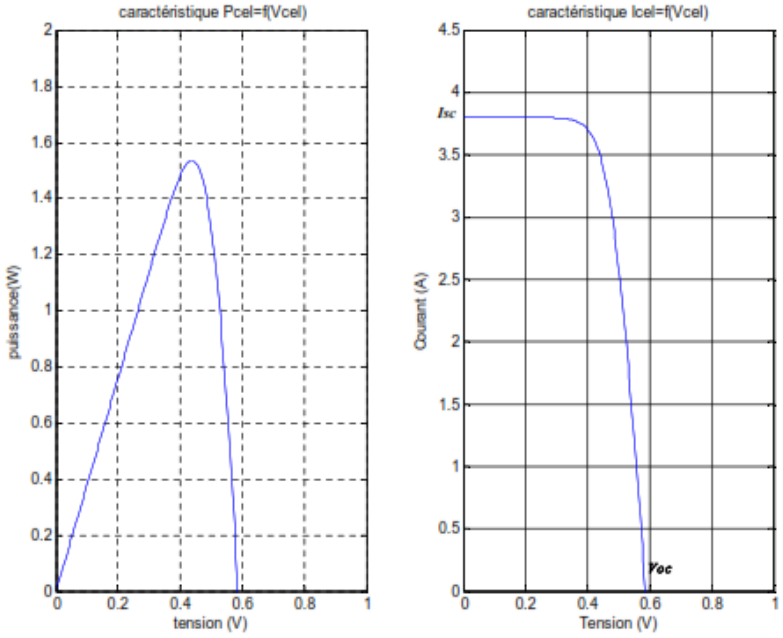

Figue I.6: Characteristic $I_{cell} = f(V_{cell})$ of a photovoltaic cell

a) Series resistance R_S:

Series resistance R_S represents the various contact and connection resistances, it is mainly due to losses by Joule effects through the collection grids and the inherent resistance of the semiconductors, as well as bad contacts (Semiconductor, such as relationship: electrodes). it plays an important role on the slope of the curve (i-v) in open circuit. In practice, the series resistance Rs is very low (of the order of a few milli-ohms). It has the relationship:

$$Rs = -\frac{dV}{dI}\Big|_{Voc,0} - \frac{1}{X_V} \quad \text{.....(I.5)}$$

$$X_{V=} = \frac{I_{s,0}}{V_{th,0}} e^{\frac{V_{oc,0}}{V_{th,0}}} \quad \text{.....(I.6)}$$

b) The saturation current Is:

The saturation current Is of the diode at a temperature T0, is given by:

$$I_{s,0} = \frac{I_{sc,0}}{e^{V_{oc,0}/V_{th,0-1}}} \quad \text{.....(I.7)}$$

It depends on the temperature. Its value for a given temperature is calculated by the equation next :

$$I_s = I_{s,0}.\left(\frac{T}{T_0}\right)^{\frac{3}{n}}.e^{-\frac{qV_g}{nk}\left(\frac{1}{T}-\frac{1}{T_0}\right)} \quad \text{.....(I.8)}$$

c) The current photo Iph.

The photocurrent Iph is directly proportional to the solar radiation E(W/m2) for a chosen temperature T0 (° Kelvin). When the cell is short-circuited, a current negligible will flow through the diode. It is given by:

$$I_{ph/T_0} = \frac{I_{sc,0}}{E_0}.E = C_1.E \quad \text{……(I.9)}$$

$$I_{ph} = \frac{I_{sc/T2} - I_{sc,0}}{T_2 - T_0} \quad \text{……(I.10)}$$

$$I_{ph} I_{ph/T_0}.(1 + k_0(T - T_0) \quad \text{.....(I.11)}$$

With K_0: temperature coefficient of Iph (usually given by the manufacturer on the datasheet as percentage change per degree Celsius).

I.4.3. External parameters of a photovoltaic cell:

These parameters can be determined from current-voltage curves, or from the characteristic equation. The most common are the following:

a) The short-circuit current I_{sc} :

This is the current for which the voltage at the cell or PV generator terminals is zero. It is directly proportional to the radiant energy received, to the ambient temperature, to the speed of circulation of the ambient air and to the surface of the cell. In the ideal case (R_s zero and R_{sh} infinite), this current merges with the photo current I_{ph}:

$I_{sc} = I_{ph}$……(I.12)

Otherwise, by canceling the voltage in equation (1.2), we obtain:

$$I_s = I_{ph} - I_0\left(e^{q\left(\frac{R_s I_{SC}}{nKT}\right)} - 1\right) - \frac{I_{sc}R_s}{R_p} \quad \text{……(I.13)}$$

b) The open circuit voltage V_{oc}

For an infinitely large load (open circuit), the output current is zero and the voltage across the cell is maximum. This voltage almost does not vary with light intensity is called open circuit voltage V_{oc} (open circuit).

From equation (I.4), we can write:

$$V_{oc} = \frac{AKT}{q} In\left(\frac{I_{ph}}{I_s} + 1\right) = V_{th} In\left(\frac{I_{ph}}{I_s} + 1\right) \quad \text{……(I.14)}$$

c) The Form Factor FF:

The form factor FF is the ratio between the maximum value of the power that can be extracted PMPP from the solar cell under standardized measurement conditions, and the product Isc, V_{oc} **[5] :**

$$FF = \frac{V_{MPP} I_{MPP}}{V_{oc} I_{sc}} \quad \text{.....(I.15)}$$

It represents the measure of the quality of the solar cell. This value for a crystalline solar cell is between 0.7 and 0.8. It decreases with increasing cell temperature.

d) The efficiency η:

Photovoltaic efficiency is a very important factor for photovoltaic components, it is defined as the ratio between the maximum power delivered by the cell P_{max} and the power of the incident solar radiation P_i.

$$\eta_m = \frac{P_{max}}{P_i} = \frac{I_m V_m}{E.S} \quad \text{.....(I.16)}$$

The performance of solar panels depends on geographic location, cloud cover, time of year, etc.

e) The characteristic power of a cell P

Under fixed ambient operating conditions; illuminance, temperature, ambient air circulation speed, etc., electrical power *P*(*W*) available at the terminals of a photovoltaic cell is equal to the product of the direct current supplied I by a direct voltage *V*.

P= Vx I.....(I.17)

P(W) : Power measured at the terminals of the photovoltaic cell;

V(V) : Voltage measured at the terminals of the photovoltaic cell;

I(A) : Current intensity measured at the terminals of the photovoltaic cell

f) The Maximum Power

The maximum power of a cell corresponds to the point for which the product of the voltage and the current intensity is maximum.

$P_{MPP} = V_{MPP}. I_{MPP}$.....(1.18)

Mathematically, we get this point as follows:

$$\frac{\partial P}{\partial V} = \frac{\partial (IV)}{\partial V} = I + V\frac{\partial I}{\partial V} = 0 \quad \text{.....(I.19)}$$

I.5. Photovoltaic module:

The PV cells are connected in series to form the photovoltaic module, the photovoltaic module is generally consists of 36 cells in series.

Several modules form a photovoltaic panel, several panels form a photovoltaic field**.**

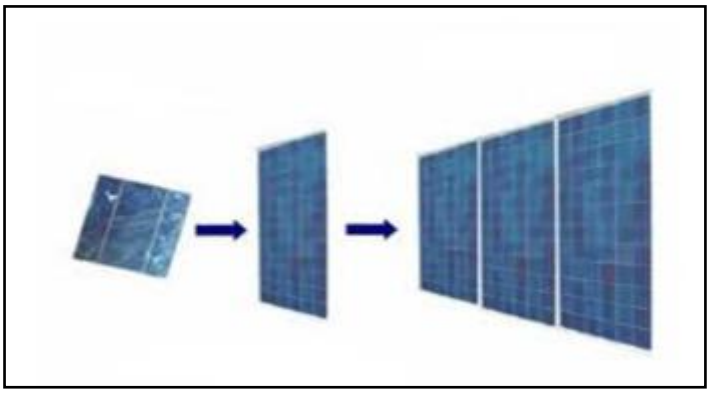

Figue I. 7 : a cell, a module and a photovoltaic panel

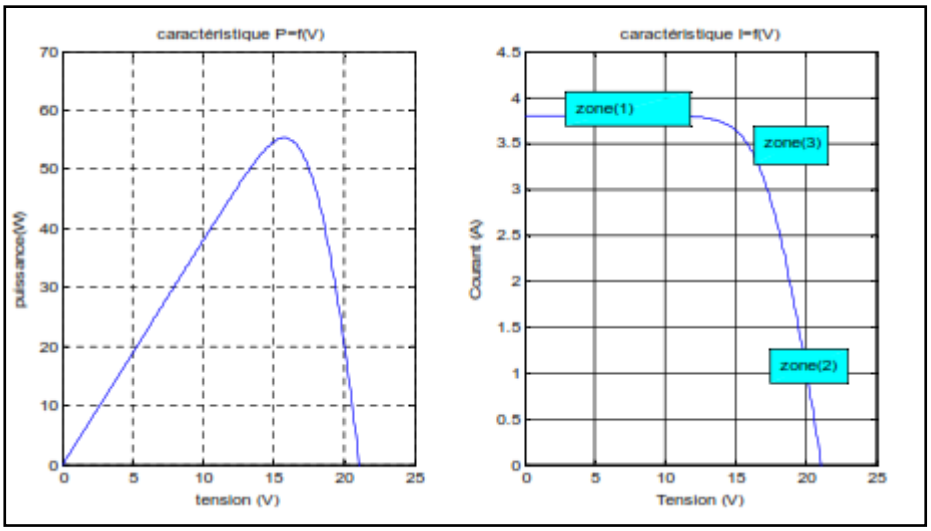

Figue I. 8: Characteristic I= f(V) of a photovoltaic module and operating zones

The operation of the module is essentially characterized by three areas:

- Zone 1: The current I is given almost constant the module behaves like a current generator (practically constant with a value close to I_{sc}). The operation of the module in this zone is characterized by: low powers, high currents and low voltages.

- Zone 2: Region corresponding to high values of R_{sh}**.** the module behaves like an open circuit voltage generator Voc. The operation of the module in this zone is characterized by: low powers, small currents and high voltages.

- Zone 3: The operation of the module in this zone is characterized by high powers, currents and acceptable voltages [6] it corresponds to the elbow of the characteristic, it is the intermediate region between the two previous zones, it represents the preferred region for generator operation where the optimum point (characterized by maximum power) can be determined.

I.5.1. Grouping of photovoltaic cells in parallel:

A parallel association of (NP) cell Figue (9) is possible and makes it possible to increase the output current of the generator thus created. In a group of identical cells connected in parallel, the cells are subjected to the same voltage and the resulting characteristic of the group is obtained by addition of the currents [7].

With:

$I_{scNP} = N_p.I_{sc}$ ……(I.20)

$V_{oc} = V_{ocNP}$……(I.21)

I_{scNP}: The sum of short circuit currents of (N_P) cell in parallel.

V_{ocNP}: The open circuit voltage of (N_P) cells in parallel.

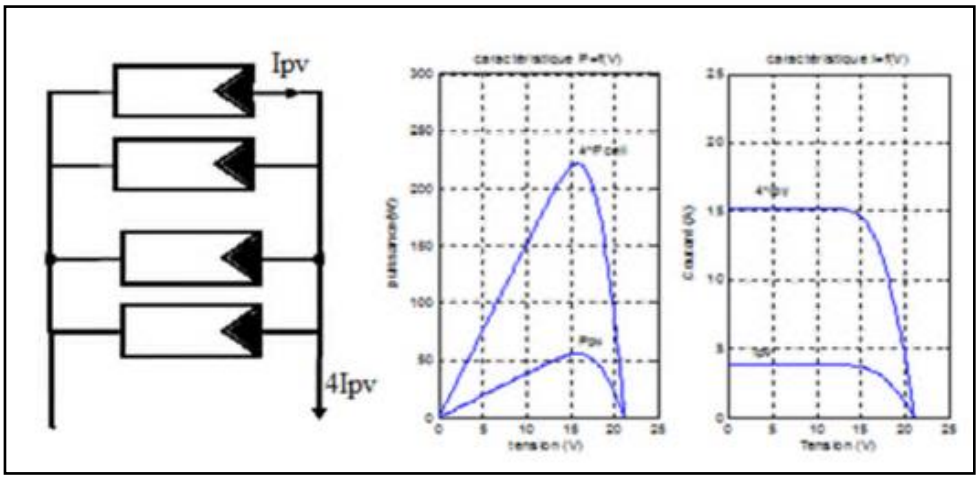

Figue I.9 : Characteristic of number of modules in parallel

I.5.2. Grouping of photovoltaic cells in series:

An association of (Ns) cells in series in Figue (10) makes it possible to increase the voltage of the photovoltaic generator. The cells are then traversed by the same current and the characteristic resulting from the series grouping is obtained by adding the elementary voltages of each cell. The equation summarizes the electrical characteristics of a series association of (Ns) cells [8].

$V_{ocNS} = N_s.V_{oc}$ ……..(I.22)

$I_{scNS} = I_{sc}$ ……(I.23)

V_{ocNS} = The sum of the open circuit voltages of Ns cells in series.

I_{scNS} = The short-circuit current of Ns cells in series.

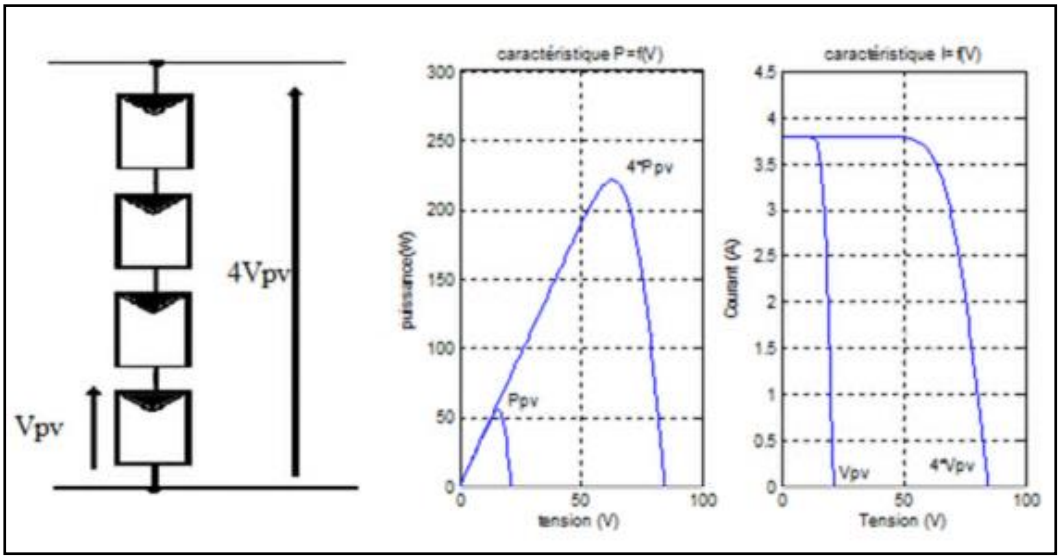

Figue I.10 : Characteristic of number of modules in series conclusion

The modules can also be connected in series and in parallel in order to increase the voltage and the intensity of use.

$P_{générateur} = N_{ms}.N_{BP}.P_{module}$ ……..(I.24)

$V_{générateur} = N_{ms}.V_{module}$ ……..(I.25)

$I_{générateur} = N_{BP}.I_{module}$ ……..(I.26)

$R_{s\ générateur} = R_S\ moudule\ \frac{N_{ms}}{N_{BP}}$ ……..(I.27)

Ou:

N_{ms} : Number of modules associated in series.

N_{BP}: Number of parallel branches.

I.6. Effects of Climatic Variations on the Photovoltaic module:

I.6.1. Influence of illumination:

illustrates the variation of the power delivered by the generator as a function of the voltage for different values of illumination, which allows us to dedication the influence of illumination on the P(V) characteristic [9].

shows the influence of illuminance on the characteristic *I=f(V)*. At a constant temperature, we see that the current undergoes a significant variation, but by against voltage varies slightly. Because the short-circuit current is a linear function of illuminance while open circuit voltage is a logarithmic function [10.11]

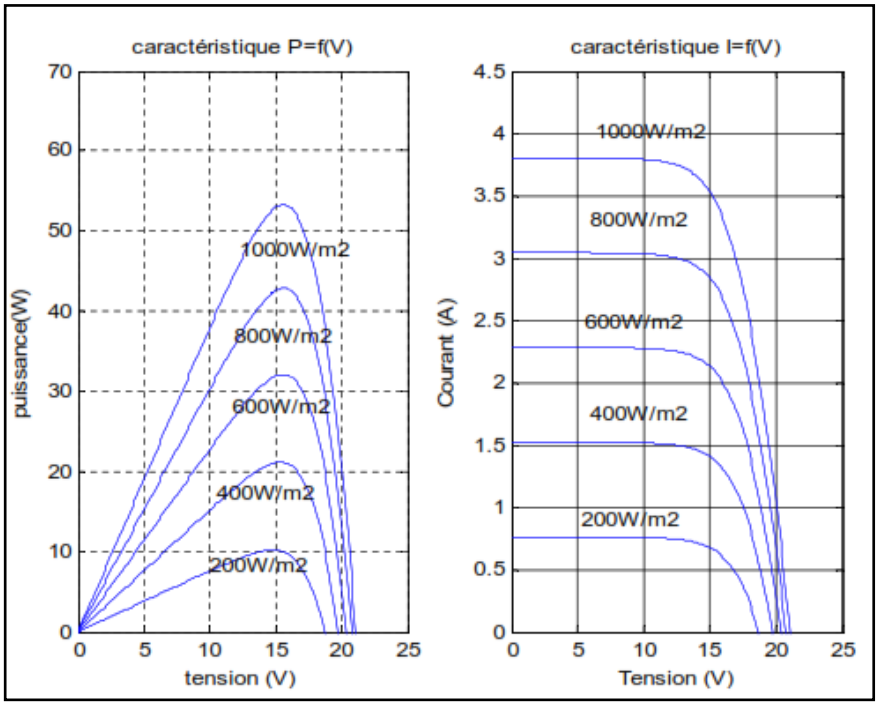

Figue I.11: The influence of illumination on P=f(V), et I=f(V)

I.6.2. Influence of temperature

illustrates the variation of the power delivered by the generator as a function of the voltage for different values of the temperature, which allows us to deduce the influence of the temperature on the characteristic P(V) [10].

shows the influence of temperature on the characteristic *I=f(V)*.

Il est essentiel de comprendre l'effet de changement de la température d'une cellule solaire sur la caractéristique *I=f(V)*.

The current depends on the temperature since the current increases slightly as the temperature increases, but the temperature negatively influences the circuit voltage opens. As the temperature increases the open circuit voltage decreases. Therefore the maximum power of the generator undergoes a decrease [11]

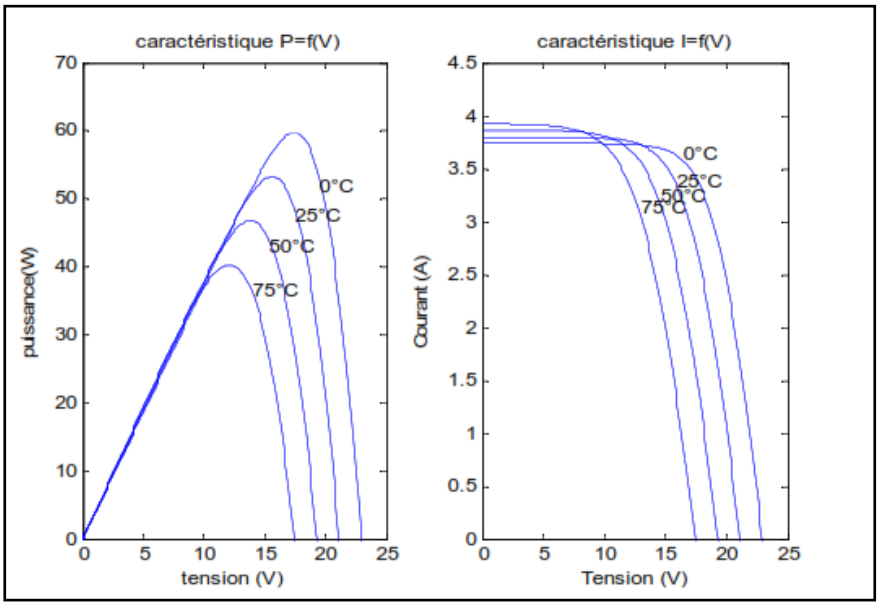

Figue I.12 : The influence of temperature on the characteristics P=f(V), et I=f(V)

I.7. Applications of photovoltaic energy:

Apart from space applications at the origin of the development of photovoltaic techniques and applications in electronics (supply of calculators, watches,

etc.), there are two main families of applications, namely:

I.7.1. Standalone apps:

For supplying sites isolated from the electricity distribution network (housing, microwave relay, pumping, beaconing at sea, rural electrification, etc.);

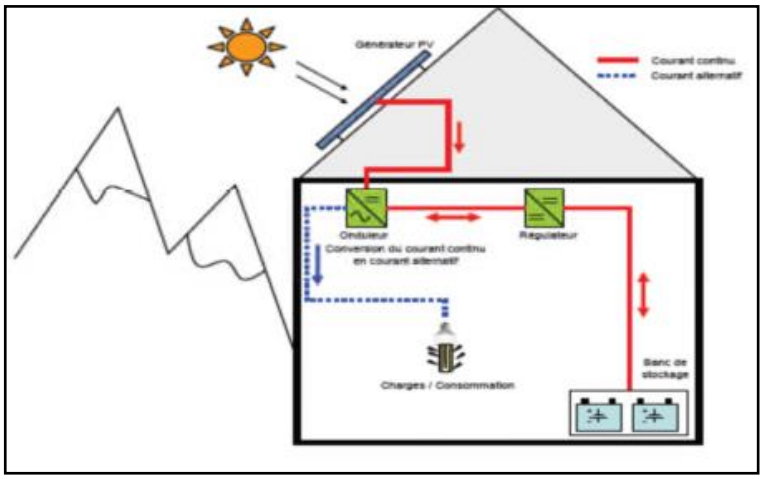

Figue I.13 : Example of the structure of a stand-alone PV system

I.7.2. Non-standalone applications:

It is possible to use a photovoltaic generator in a non-autonomous way, by connecting it to the public electricity distribution network. We will then have a small electricity production plant, the energy of which will either be consumed on site by the owner, or sold on the network. In the event of excess production, the photovoltaic generator supplies the network and conversely, the network supplies the distribution in the event of a deficit or out of solar generation. The whole is fully automated and managed by one or more inverters.

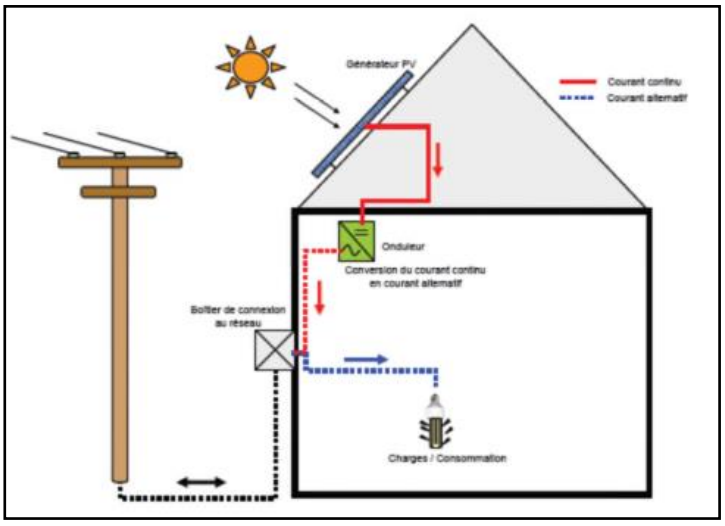

Figue I.14: Example of the structure of a PV system connected to the network

I.8. Direct connection (load source):

The simplest system that can be designed consists of a photovoltaic generator (GPV) and a continuous type load (DC) which directly uses the power supplied by the GPV. This power strongly depends on the illumination, the temperature and the nature of the load. The direct connection between the photovoltaic panel and the load is widespread due to its simplicity of implementation, as well as its minimal cost due basically to the absence of electronics except for a blocking diode sometimes necessary to avoid a possible return of the current (Figue 15).

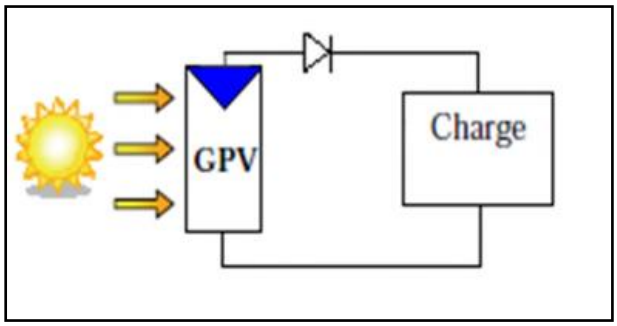

Figue I.15 : Direct source-load connection

Unfortunately this configuration does not offer any 'tuning' parameters. The power supplied by the photovoltaic module is fixed by the intersection between the current-voltage (I-V) characteristic of the GPV and that of the load. The power transfer will therefore not be able to remain optimized when the characteristics fluctuate.

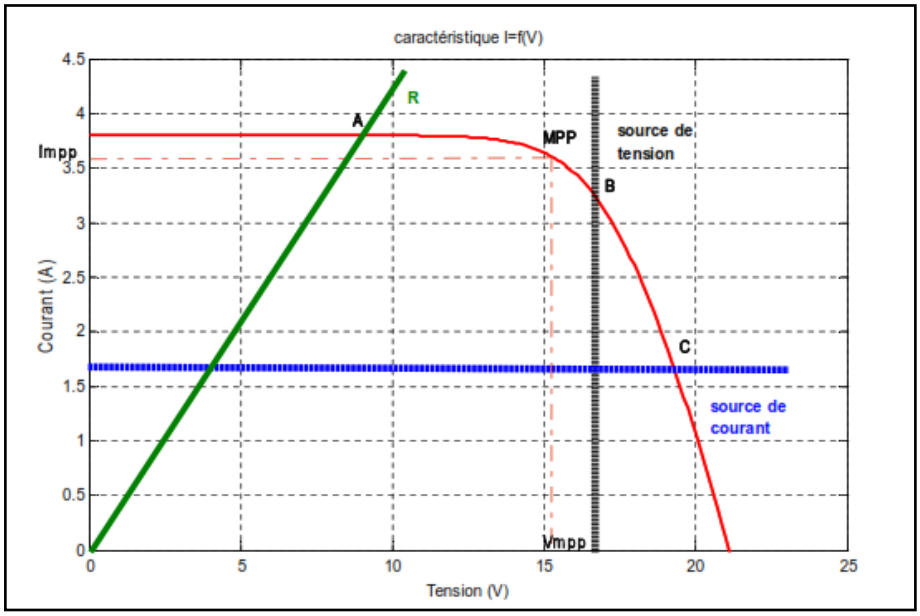

Figue I.16 : GPV operating points in direct connection to the load.

More generally, a GPV can be connected directly to three types of loads:

- A DC voltage source type load,
- A direct current source type load,
- A purely resistive load.

In Figue I.18, the I(V) and P(V) characteristics of a GPV are schematized thus the operating point where the power supplied by the generator is maximum
(P_{MAX}) corresponds to the operating point *PPM* (I_{OPT}, V_{OPT}). The points of intersection between the electrical characteristic of the GPV and that of the different loads are respectively

- Point A for a purely resistive load.
- Point B for a DC voltage source type load,
- Point C for a direct current source type load,

As previously illustrated there are three respective operating points A, B, C
can be identified providing power P_A, P_B et P_C. These Figues show that the GPV is poorly exploited and does not provide the maximum power [12].

I.9. Advantages and disadvantages of a PV installation:

a) Advantages

- first, high reliability. The installation has no moving parts which makes it particularly suitable for remote areas. This is the reason for its use on spacecraft.
- then, the modular nature of the photovoltaic panels allows a simple assembly and adaptable to various energy needs. Systems can be sized for power applications ranging from milliwatts to megawatts.
- the operating cost is very low given the reduced maintenance and it does not require fuel, transport or highly specialized personnel.
- photovoltaic technology has qualities from an ecological point of view because the finished product is non-polluting, silent and does not cause any disturbance of the environment, except by occupying space for large-scale installations [3].

b) Disadvantages

- the manufacture of the photovoltaic module is high technology and requires high cost investments.
- the actual conversion efficiency of a module is low, around 10-15%, with a theoretical limit for a cell of 28%. Photovoltaic generators are competitive with diesel generators only for low power demands in remote areas.

- the low efficiency of photovoltaic panels is explained by the very functioning of the cells. To be able to move an electron, the energy of the radiation must be at least equal to 1 eV. All the incident rays having a lower energy will therefore not be transformed into electricity. Similarly, light rays with an energy greater than 1 eV will lose this energy, the rest will be dissipated as heat.
- dependent on weather conditions.
- when the storage of electrical energy in chemical form (battery) is necessary, the cost of the generator is increased.
- the storage of electrical energy still poses many problems.

I.10. Conclusion

This chapter, divided into two parts, first allowed us to define the different sources of global energy; namely renewable and non-renewable energies considering that solar energy is the energy of the future.

Secondly, we presented an overview of photovoltaic energy, the operating principle of a photovoltaic cell, the use of its current-voltage characteristic to calculate its various physical parameters. We have also seen the effect of climate change on the characteristic $I=f(V)$ from *GPV*.

In addition, its operating point depends on the load it supplies. In order to extract at all times the maximum power available at the terminals of the GPV, we introduce an adaptation stage between the generator and the load, hence the purpose of the second chapter.

CHAPTER II

STUDY OF DC/DC CONVERTERS

II-1. Introduction

A GPV exhibits nonlinear I-V characteristics that admit a single point optimal operating conditions in homogeneous lighting and lighting conditions temperature. An impedance adaptation is necessary and this can be done by a direct coupling of a suitable load or by inserting between the GPV and the electrical load an electronic device.

This device is nothing other than a static converter equipped with a control of continuation of the PPM.

In order to design a more efficient power interface, a study detailed is made on the static DC-DC converters not isolated in mode of continuous conduction. The design of an adaptation stage equipped with an MPPT algorithm makes it possible to optimize energy conversion and easily connect a GPV to its load. In this chapter, we are interested in the study of the Buck-Boost type DC/DC converter as energy conversion stage, we will present some existing MPPT techniques which allow the GPV to operate at its maximum power.

II.2. DC/DC converters

Choppers are DC-DC type converters for controlling electrical power in circuits operating on DC with great flexibility and high efficiency.

The chopper consists of capacitors, inductor and switches. In the ideal case, all these devices do not consume any active power, which is why we have good yields for choppers [13].

II.2.1. Step-down chopper (Buck)

A Buck converter, or series chopper, is a switching power supply that converts a DC voltage into another DC voltage of lower value. This type of converter is used for applications that can be classified into two categories:

•Applications aiming to obtain a fixed (and sometimes regulated) DC voltage from a higher DC voltage generator.

•Applications to obtain an adjustable voltage but always lower than that present at the input [14].

Figue (II.1) shows the block diagram of the buck converter.

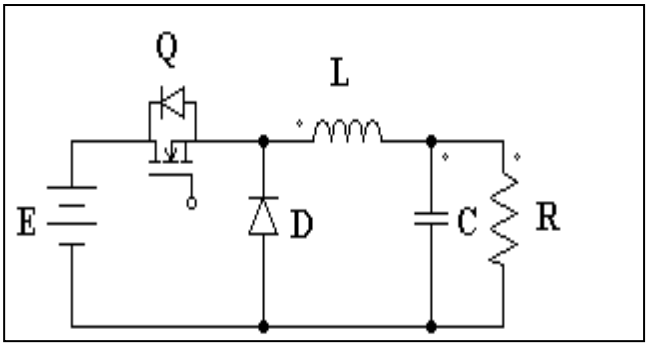

Figue II.1. Real buck conv

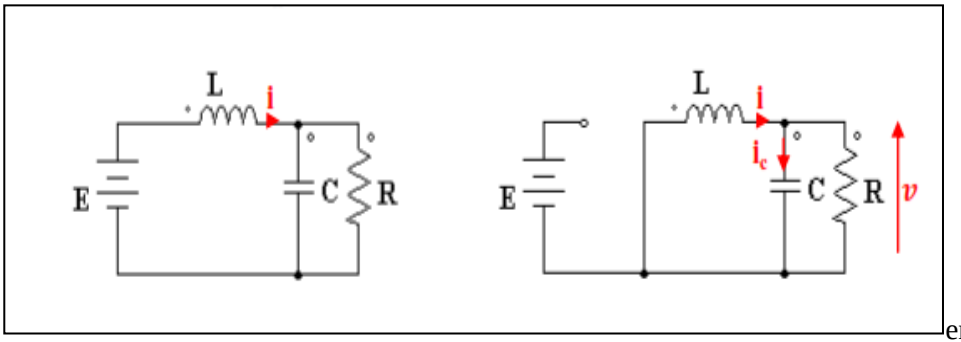

erter.

(a) *Switch in position u= 1.* ***(b)*** *Switch in position u= 0.*

Figue II.2. Circuit buck converter topologies.

a) If we consider that the switch is closed (u=1) and by applying the laws of Kirchhoff to the circuit we obtain the following equations:

$L\frac{di}{dt}$= E-V……...…….(II.1)

$C\frac{dv}{dt}$ = I - $\frac{v}{R}$ …….(II.2)

b) For u=0 (the switch open):

$L\frac{di}{dt}$= -V……...…….(II.3)

$C\frac{dv}{dt}$ = I - $\frac{v}{R}$ ……..…….(II.4)

By comparing the two situations we can obtain a single unified model which is:

$L\frac{di}{dt}$= uE - V…….(II.5)

$C\frac{dv}{dt} = i - \frac{v}{R}$ ……..……..…….(II.6)

The average model of the buck converter is described by:

$L\frac{di}{dt} = Eu_{av} - v$……..…….(II.7)

$C\frac{dv}{dt} = i - \frac{v}{R}$ ……..…….(II.8)

Using normalization:

$x_1 = \frac{i}{E}\sqrt{\frac{L}{C}}$; $x_2 = \frac{v}{E}$; $\tau = \frac{t}{\sqrt{LC}}$; $Q = R\sqrt{C/L}$ ……(II.9)

We then obtain the following normalized mean model:

$\frac{dx_1}{d\tau} = - X_2 + u_{av}$ ……...……...….(II.10)

$\frac{dx_2}{d\tau} = X_1 - \frac{x_2}{Q}$ ……...……...…….(II.11)

II.2.1.1. Composition of the converter

a) The MOSFET transistor

The low-power MOSFET (Metal Oxide Semiconductor Field Effect Transistor). Figue (II.1.a) gives the usual symbolic representation. The connection starting from the terminal linked to the substrate (buck) B ends with an arrow indicating the passing direction of the two substrate-source and substrate-drain junctions.

Usually the substrate and the source are connected. Figue (II.2.b) indicates the notations used.

In a P-type doped semiconductor (Figue II.3), two N-type zones have been diffused onto which are soldered the two source S and drain D contacts. An oxide layer covers the P zone located between source and drain; on this layer is welded the gate contact (gate) G. It is the succession Metal-Oxide-Semi-conductors which gives the prefix MOS used to characterize this type of transistor [15].

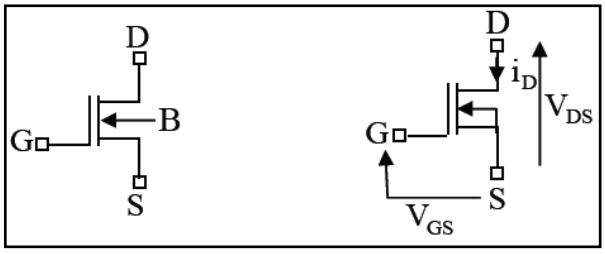

(a) (b)

Figue II.1. Symbolic representation and notation for the N-channel MOSFET.

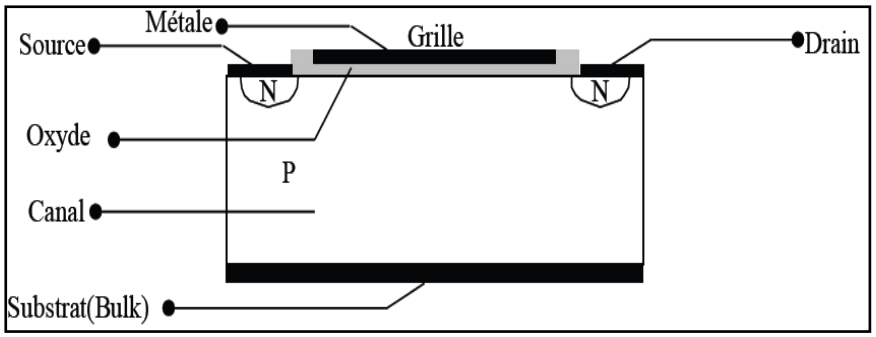

Figue II.2. Structure of a low-power MOSFET cell

The use of the MOSFET transistor offers several advantages:

- Intrinsic noise is still very low.
- This type of transistor is simple to manufacture and subsequently inexpensive.
- The integration density authorized by this type of component is very high:

today we exceed the number of 107 transistors on a single chip.

b) The capacitor

The capacitors that we encounter in switched-mode power supplies fulfill two distinct roles: they serve as energy during command or load variations, and they also serve as switching or filtering capacitors with respect to the high-frequency operation of food. These are the so-called low series resistance chemical capacitors which have high capacitance values, while having excellent frequency resistance. The capacitor is characterized by physical quantities which define its fields of application. The capacitance of a capacitor is equal to the ratio of the electric charge Q stored to the voltage V applied between its plates.

C(F) = Q(C)/V (V) ……..……..….(II.12)

In the simplified case of a capacitor whose surface S of the opposite plates is

Plane, the expression of the capacity is:

C= $\varepsilon_r \varepsilon_0 \, S/e$……..……..…….(II.13)

With :

ε_0 : Permittivity of vacuum.

ε_r: Relative permittivity (2 to 20000) of the dielectric.

e: thickness of the dielectric [15].

c) Inductance

The role of an inductor is to store electrical energy in magnetic form, then to release it. It is of course possible to produce air coils.

But, the use of magnetic circuits as presented below allows:

1. to reduce bulk, with the same inductance value.
2. to confine the magnetic flux in a restricted space and thus to limit parasitic radiation.

Inductors are mainly used in filtering, energy conversion (switching power supplies, etc.) and magnetic switches (saturable inductors) applications. The equivalent circuit diagram of a simple inductor L is the following:

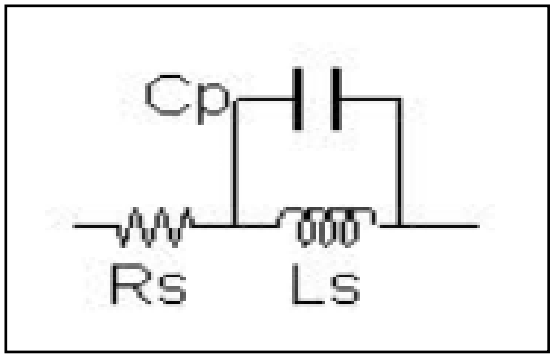

Figue II.3. single inductor L.

where Rs represents the series resistance of the wound wire and Cp the inter-turn parasitic capacitances.

The value of the inductance is obtained by:

$$L = \mu_0 \mu_e \frac{S_e}{l_e} N^2 \quad \text{(II.14)}$$

Avec:

$\mu_0 = 4\pi\ 10^{-7}$(SI)

μ_e : relative permeability (including between possible iron).

S_e: magnetic effective section of the core (average section).

Effective magnetic length (average length of the magnetic circuit)

N: number of turns [15].

d) Schottky diode

The Schottky diode has two advantages over conventional diodes:

- Electrical characteristic: 600 V blocking voltage.
- Lower threshold voltage (Vs = 0,3V).
- Schottky diodes have very short reverse recovery times (tr from 0.15 to 0.35µs).
- Schottky diode applications

Schottky diodes are used at low voltage in circuits requiring high switching speed, for example in high-frequency chopper assemblies found in switched-mode power supplies [15].

I1.2.2 Boost Chopper (Boost)

A Boost converter (or Step-Up in English), or parallel chopper, is a switching power supply that converts a DC voltage into another DC voltage of higher value. A Boost converter is used when you want to increase the voltage available from a continuous source [14]. its basic block diagram is that of Figue (II.4).

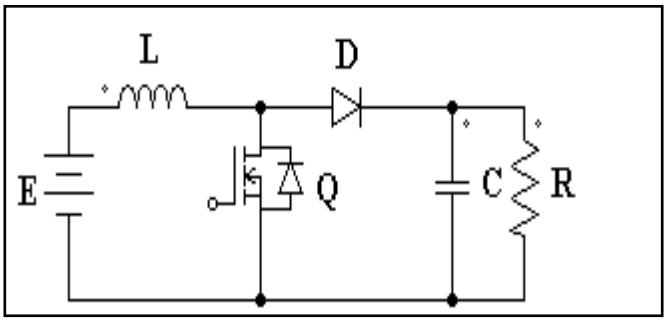

Figue II.4. Real Booster Converter.

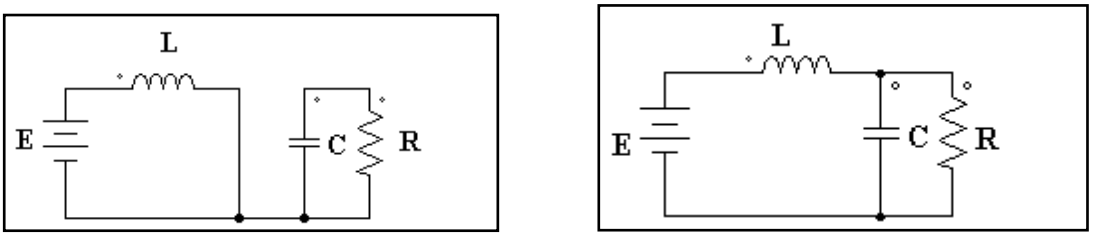

***(a)** position switch u= 1* ***(b)** position switch u= 0*

Figue II.5. Circuits of the boost converter topologies.

a) If we consider that the switch is closed (u=1) and by applying the laws of Kirchhoff to the circuit we obtain the following equations

$L\frac{di}{dt}= E$……(II.15)

$C\frac{dv}{dt} = -\frac{v}{R}$……(II.16)

b) When the switch is open (u=0) the following dynamic is obtained:

$L\frac{di}{dt}= E - V$……(II.17)

$C\frac{dv}{dt} = i -\frac{v}{R}$……(II.18)

By comparing the two situations we can obtain a single unified model which is:

$L\frac{di}{dt}= E - (1-u)v$……(II.19)

$C\frac{dv}{dt} = (1 - u)\, i -\frac{v}{R}$……(II.20)

Using normalization:

$x_{2=\frac{i}{E}}\sqrt{\frac{L}{C}}$; $x_2 = \frac{v}{E}$; $\tau = \frac{t}{\sqrt{LC}}$; $Q=R\sqrt{C/L}$ ……(II.21)

We then obtain the following normalized mean model:

$\frac{dx_1}{d\tau} = 1- (1 - u_{av})x_2$……(II.22)

$\frac{dx_2}{d\tau} = (1 - u_{av})x_1 - \frac{x_2}{Q}$ ……(II.23)

II.2.3Buck-Boost chopper

A Buck-Boost converter is a switching power supply that converts a DC voltage into another DC voltage of lower or higher value but of opposite polarity. A disadvantage of this converter is that its switch does not have a terminal connected to ground, thus complicating its control [14]. Figue (II.6) presents the block diagram of the Buck-Boost converter.

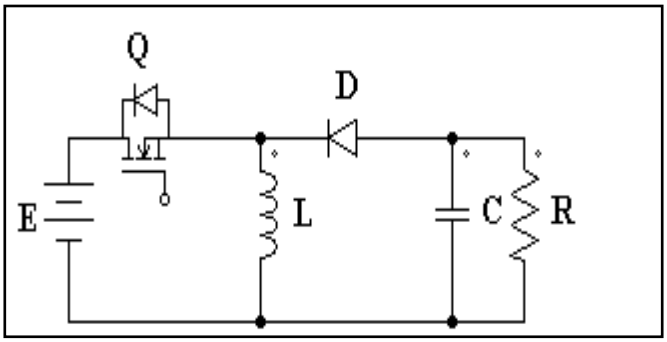

Figue II.6. Real buck-boost converter.

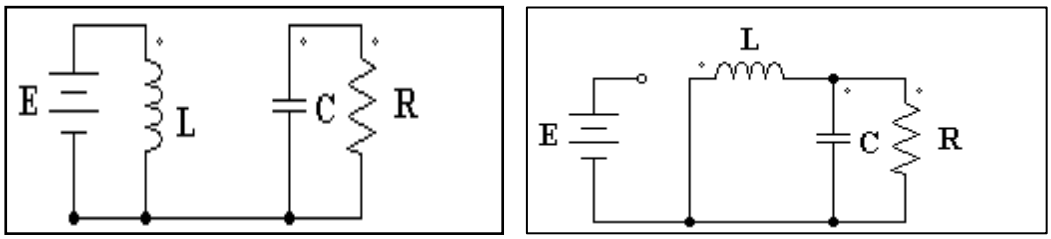

***(a)** Position switch u= 1* ***(b)** position switch u= 0*

Figue II.7. Circuits of Buck-Boost converter topologies.

a) If we consider that the switch is closed (u=1) and by applying the laws of Kirchhoff to the circuit we obtain the following equations:

$L\frac{di}{dt} = E$……..…….(II.24)

$C\frac{dv}{dt} = -\frac{v}{R}$……..…….(II.25)

a) When the switch is open (u=0) the following dynamic is obtained:

$L\frac{di}{dt} = V$……...……...…….(II.26)

$C\frac{dv}{dt} = -i - \frac{v}{R}$…….(II.27)

By comparing the two dynamics, we obtain the following switched model:

$\frac{di}{dt} = 1-(1-u)v+uE$ ……..……..…….(II.28)

$\frac{dx_2}{d\tau} = -(1-u)u - \frac{v}{R}$ …….….(II.29)

Using normalization:

$x_{2=}\frac{i}{E}\sqrt{\frac{L}{C}}$; $x_2 = \frac{v}{E}$; $\tau = \frac{t}{\sqrt{LC}}$; $Q=R\sqrt{C/L}$ ……..……..(II.30)

Then the normalized mean model is:

$\frac{dx_1}{d\tau} = (1 - u_{av})x_2 + u_{av}$ ……..…….(II.31)

$\frac{dx_2}{d\tau} = -(1 - u_{av})x_1 - \frac{x_2}{Q}$ ……..…….(II.32)

II.3. Principle of operation of the DC-DC converter for the MPPT tracking

The chopper or DC-DC converter is a power electronics device which can be made using electronic switches that can be opened and closed, such as: the bipolar transistor (BJT), the transistor field effect (FET) or insulated gate (IGBT) operating in switching mode. The principle of the chopper consists in establishing then periodically interrupting the underload connection using the electronic switch. This must be able to be closed or opened at will (the

control) in order to have an adjustable continuous output voltage from a fixed continuous input voltage.

Choppers are used in solar power systems for finding the maximum power point. However, there are different types of DC-DC converters that are frequently used in such applications, such as the "step-down" series chopper, the "boost" parallel chopper or the series-parallel chopper which is a combination of the two previous ones.

II.3.1. Hacheur série ou abaisseur (Buck).

This name is related to the fact that the average output voltage is lower than that of the input.

It comprises a switch with priming and blocking commands and a switch with blocking and spontaneous priming (diode). Figue (II.8) shows the block diagram of a step-down converter.

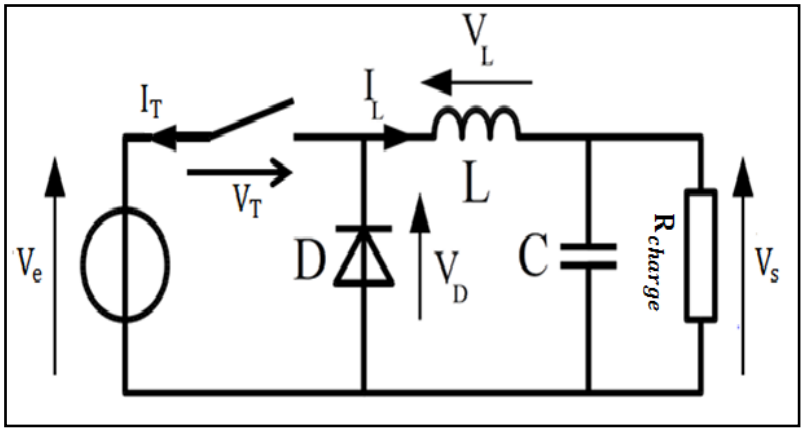

Figue. II.8. Block diagram of a step-down chopper (Buck)

It is characterized by the transformation ratio (in continuous conduction).

This type of converter is not desirable for the search for the maximum power point in the case of high powers, moreover its control is very complex.

II.3.2. Parallel Chopper or Booster (Boost)

In this type of chopper, the average output voltage is higher than the input voltage, hence its name. This structure requires a control switch with ignition and blocking and a diode with spontaneous ignition and blocking. Figue (II.9) shows the scheme.

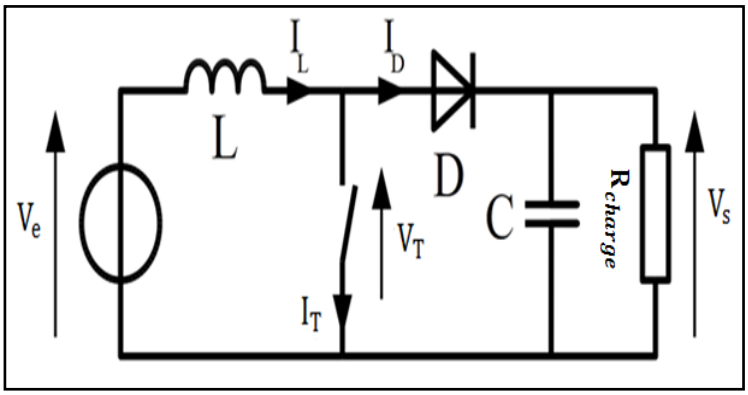

Figue. II.9. Block diagram of a step-up chopper (Boost)

It is characterized by the transformation ratio (in continuous conduction)

type of converter is not desirable for finding the maximum power point $M(\alpha) = \frac{V_s}{V_e} = \frac{1}{1-\alpha}$ Ce

in the case of low powers.

II.3.3. Series-Parallel or Buck-Boost chopper

This type of chopper is nothing other than a switching power supply which converts a DC voltage into another DC voltage of lower or higher value, but of polarity reverse. Figue (II.10) gives the basic diagram of a buck-boost converter.

It is characterized by the transformation ratio (continuous conduction) $M(\alpha) = \frac{V_s}{V_e} = \frac{1}{1-\alpha}$ Ce

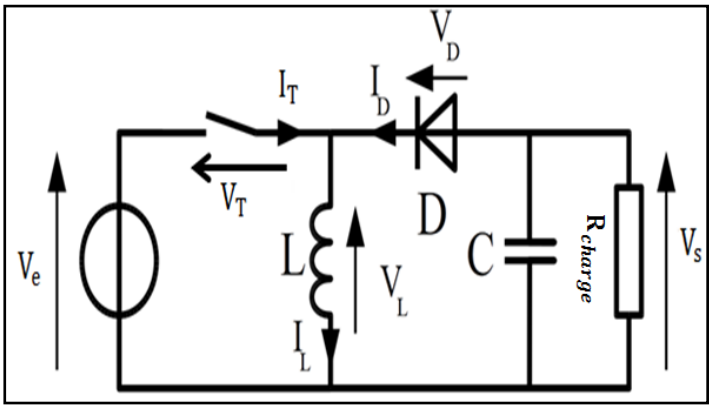

Fig. II.10. Block diagram of a step-down chopper (Buck-Boost)

The disadvantage of this type of converter is that its switch does not have

terminal connected to zero, thus complicating its control. However, it remains the type of converter which is most suitable for a good search for the maximum power point, whether at low or high power.

II.4. Buck-Boost Converter Analysis

II.4.1. Functioning

There are two modes of operation of the converter which depend on the conduction of the current in the coil:

• a continuous conduction mode where the current is never cancelled.

• a discontinuous conduction mode where the current is periodically cancelled.

In our application, we will use the 1st mode. From now on, all the given relations which will be used are only valid for the continuous mode of conduction. The in the Figue (II.11).

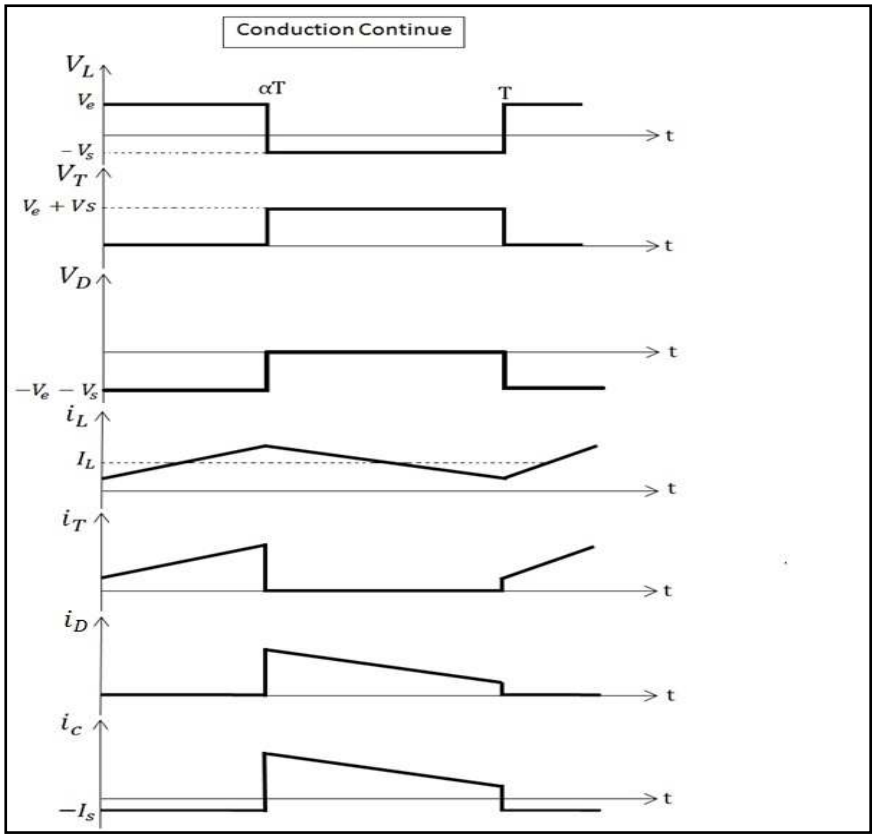

Figue. II.11. Buck-Boost Chopper Waveforms

During the first phase of the operating cycle, from 0 αT (α is the duty cycle of the control signal and T is its period), the control switch is closed, the diode is open and the coil stores the energy supplied by the input generator. We'll have:

$$V_L = V_e = L\frac{di_L}{dt} \quad \text{……..……...…….(II.33)}$$

With $i_T = i_L$

And: $i_s = 0$

From where:

$$i_L = \frac{V_e}{L}t + I_{L\,Max} = \frac{V_e}{L}\alpha T + I_{L\,Min} \quad \text{.....(II.34)}$$

During the second phase of the operating cycle, from αT to T, the control switch is open and the diode becomes conductive, the coil then restores its energy to the load. We'll have :

$$V_L = -V_e = L\frac{di_L}{dt} \quad \text{.....(II.35)}$$

With $i_s = 0$

And: $i_T = i_L$

From where:

$$i_L = \frac{-V_e}{L}(t - \alpha T) + I_{LMax} \rightarrow I_{LMin} = \frac{-V_s}{L}(1-\alpha)T + I_{LMax} \quad \text{..... (II.36)}$$

Note that the direction of the output voltage and current is inverse.

II.4.2. Calculation of Buck-Boost quantities

In continuous conduction mode, the following quantities can be calculated:

• Average output voltage:

We know that the average voltage at the terminals of the inductor is always zero so we have, in continuous conduction, the average value of the output voltage:

$V_e\,\alpha T = V_s(1-\alpha)\,T$ .....(II.37)

$$V_s = \frac{\alpha V_e}{1-\alpha} \quad \text{.....(II.38)}$$

Depending on the value of α, the average output voltage may be higher or lower than the input voltage, hence the name of boost-buck chopper sometimes given to this assembly.

• Average output current:

On Id = Is because the average current in the capacitor is always zero. From where:

$I_s = (1+\alpha)\,I_L$ .....(II.39)

Moreover, knowing the average output voltage and the resistance of the load, we deduce easily Is which allows to know IL.

• Current ripple in the coil:

The peak-to-peak ripple of the current in the coil:

$$\Delta i_L = I_{L\,Min} \quad \text{.....(II.40)}$$

By replacing (II.8) and (II.9) in (II.10) we will have:

$$\Delta i_L = \frac{V_e}{L}\alpha T + I_{LMax} + \frac{V_s}{L}(1-\alpha)T + I_{LMax} \quad \text{.....(II.41)}$$

We therefore obtain:

$$\Delta i_L = \frac{V_s(1-\alpha)}{L*\mathrm{f}} = \frac{V_e\alpha}{L*\mathrm{f}} \quad \text{(II.42)}$$

This ripple makes it possible to size the inductance L to ensure the conduction mode keep on going.

• Output voltage ripple:

Another capacitor Cs is needed to filter the output voltage. It obeys the classic dimensioning rules in power electronics. Load variation

ΔQ in this capacitor during a switching period is the area of the rectangle in the first phase from 0 to αT (Fig. II.10). It is given by:

$\Delta Q = \alpha T * I_s$ ……(II.43)

The charge-voltage relationship is given by:

$\Delta Q = C_s * \Delta V_s$ …….. (II.44)

By combining the two equations (II.40) et (II.41), on aura :

$$\alpha T * I_s = C_s * \Delta V_s \rightarrow C_s = \frac{\alpha T I_s}{\Delta V_s} \quad \text{(II.45)}$$

On the other hand we have:

$$I_s = \frac{V_s}{R_{charge}} \quad \text{(II.46)}$$

By replacing (II.16) in (II.15) we find:

$$C_s = \frac{\alpha V_s}{\Delta V_s * R_{charger} * \mathrm{f}} \quad \text{(II.47)}$$

• Input voltage ripple:

In photovoltaic applications, it is mandatory to add a high value capacitor at the input of the DC-DC converter to protect the photovoltaic generator from high frequency oscillations, generated by the switching of the converter. The sizing of this capacitor can be done as follows:

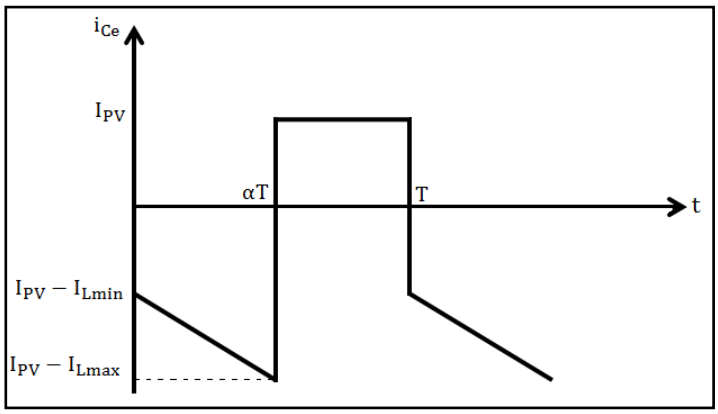

Figue. II.12. The shape of the current flowing through the input capacitor

From equation (II.41) we have:

$\Delta Q = C_e * \Delta V_e$ ……..(II.48)

We calculate the area of the shape of the current in the interval [0 αT] (Fig. II.11) which represents the

amount of charge ΔQ.

$\Delta Q = \frac{\alpha V_s}{R_{charger} * f}$ ……..……. (II.49)

By combining equations (II.18) and (II.19) we find:

$C_e = \frac{\alpha V_e}{\Delta V_e * R_{charger} * f}$ ……..……(II.50)

II.4.3. Sizing of the Buck-Boost converter

Before starting the task of sizing the various components of the converter, it is first of all important to determine the specifications of the overall system.

For our case, these specifications include, among other things, the technical characteristics of the solar panel to be used, the range of variation of the input voltage, the output voltage, the load current, the voltage ripples in the output, the type and value of the load, the frequency of the switching signal, the range of variation of the duty cycle, etc.

has. Characteristics of the photovoltaic panel The panel that we are going to use in our work is referenced by SLK60P6 from Siliken.

The variation intervals of its electrical output quantities are given in the following table:

Open circuit voltage	**V_{co}**	37.4	V
short circuit current	**I_{cc}**	7.5	A
Power voltage Maximum	**V_{ppm}**	30.6	V
power current maximum	**I_{ppm}**	6.87	A
Maximum power (In the STCs)	**P_{ppm}**	210.22	W

Table II. Electrical characteristics of the SLK60P6 panel from Siliken.

The photovoltaic panel used contains 60 cells in series with 3 bypass diodes. The choice of the value of the output voltage depends on what we want to do (specifications).

For our application we chose it equal to 30V (we take a resistive load

R=10Ω).

$V_e = V_{ppm} = 30.6\ V_{et}\ V_s = 30V$

Applying equation (II.8), we find:

$$\alpha_{optimal} = \frac{V_s}{V_s+V_e} = \frac{30}{30+30.6} = 0.495$$

$$I_s = \frac{V_s}{R_{charge}} = \frac{30}{10} = 3A$$

Switching frequency

The switching frequency of DC-DC converters is typically in the range of 20kHz to 1MHz beyond audible frequencies, depending on the speed of the semiconductor devices. In our work, we chose to operate at a switching frequency of 20kHz.

vs. Current and voltage ripples

It has been recommended in similar studies to take a voltage ripple (input or output) equal to 10% of the overall voltage and a current ripple in the coil equal to 20% of the overall current.

We have :

$$\Delta iL = 20\%IL = 20\%\ (Ie+Is) = 20\%\ (6.87+3) = 1.974A$$

According to the equation (II.12) we will have:

$$L = \frac{V_e \alpha}{\Delta i_L \mathrm{f}} = \frac{30.6 * 0.495}{1.974 * 20 * 10^3} = 0.387\mathrm{mH}$$

This is the minimum value of the inductance which ensures the continuous conduction mode, to avoid leaving the guarantee interval, it is advisable to take a value greater than this value, we have taken it equal to 1mH.

$$\Delta V_s = 10\%\ V_s = 3V$$

According to equation (II.17):

$$C_e = \frac{\alpha V_e}{\Delta V_e * R_{charger} * \mathrm{f}} = \frac{0.495*30}{3*10*20*10^3} = 24.75\mu\mathrm{F}$$

$$\Delta V_s = 10\% * 30.6 = 3.06V$$

From equation (II.20)

$$C_e = \frac{\alpha V_e}{\Delta V_e * R_{charger} * \mathrm{f}} = \frac{0.495*30.6}{3.06*10*20*10^3} = 24.75\mu\mathrm{F}$$

II.5. Conclusion

In this chapter, we have highlighted the different types of connection GPV-load.

In a second place, we presented the most used DC/DC converters as an adaptation stage (Buck, Boost and Buck-Boost) and detailed the role of each component in the Buck-Boost converter which is used in our project.

CHAPTER III

MPPT Methods

III.1. Introduction

Photovoltaic (PV) systems find increased use in electric power technologies. The main drawbacks of PV systems are high fabrication cost and low energy-conversion efficiency, which is partly caused by their nonlinear and temperature-dependent V–I and P–I characteristics. To overcome these drawbacks, three essential approaches can be followed:

1) Improving manufacturing processes of solar arrays: many research efforts have been performed with respect to materials and manufacturing of PV arrays.
2) Controlling the insulation input to PV arrays: the input solar energy is maximized using sun-tracking solar collectors or rearranging the solar-cell configurations of PV arrays with respect to changes in environmental conditions [17].
3) Using maximum power point tracking (MPPT).

A change in the solar irradiation or the temperature results in a shift of the MPP over a wide range, Instantaneous shading conditions and ageing of PV cells also affect the MPP locus. In addition, the load electrical characteristics may also vary [18].

As previously mentioned, the MPPT is the technique that ensures that the PV panel under any change in irradiance and cell temperature conditions gives the maximum available power. In other words, there is a need to track the MPP to maximize the power drawn off from the PV panel under any circumstance that can possibly cause the system to lose regulation [19].

III.2. Need for maximum power point tracker

As seen in the PV (power vs voltage) curve of the module in the first chapter, there exists a peak power corresponding to a particular voltage and current. Since the PV module efficiency is low (13%), it is desirable to operate the module at the peak power point so that the maximum power can be delivered to the load under varying temperature and insulation conditions. Hence maximization of power improves the utilization of the solar PV module. A maximum power point tracker (MPPT) is used for this reason. A dc/dc converter (step up / step down) serves the purpose of transferring maximum power from the solar PV module to the load. A dc/dc converter acts as an interface between the load and the module Figue III.1 [20].

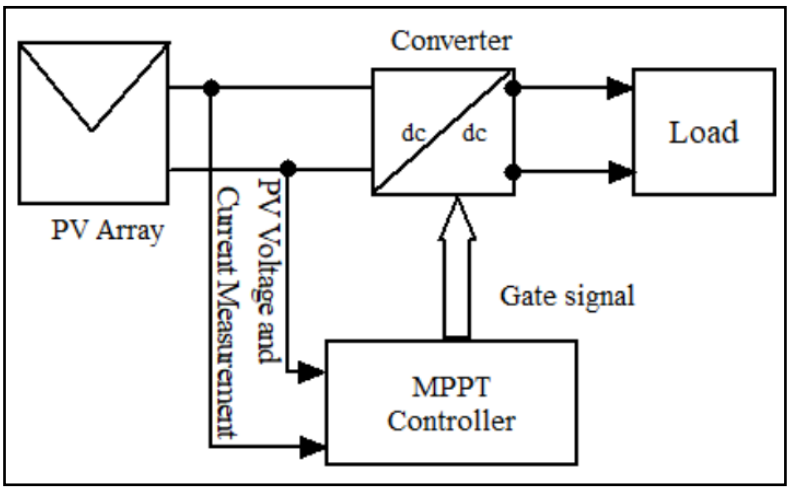

Figue III. 1: Block diagram of a typical MPPT system.

III.3 .The maximum power point tracking process

Figue III.2 illustrates the electrical characteristics of the solar array under a given insulation. The internal impedance of the solar array is low on the right side of the curve and high on the left side. The maximum power point of the solar array is located at the knee of the curve. According to the maximum power transfer theory, the power delivered to the load is maximum when the source internal impedance matches the load impedance. Thus, the impedance seen from the converter side (which can be adjusted by controlling the duty cycle) needs to match the internal impedance of the solar array if the system is required to operate close to the MPP's of the solar array. Most traditional dc/dc converters have an inherentnegative impedance characteristic, as their current increases when the voltage decreases. This behavior is due to the constant input power and the adjustable output voltage of the power supply. If the system operates on the high-impedance (namely, low-voltage) side of the solar array characteristic curve, the solar array terminal voltage will collapse. Therefore; the solar array is required to operate on the right side of the curve to perform the tracking process. Otherwise, the converter will operate with the maximum duty cycle, and the solar array voltage will only change with the insulation. Thus, the system cannot achieve maximum power tracking and might even mistake the present operating point for the MPP [21].

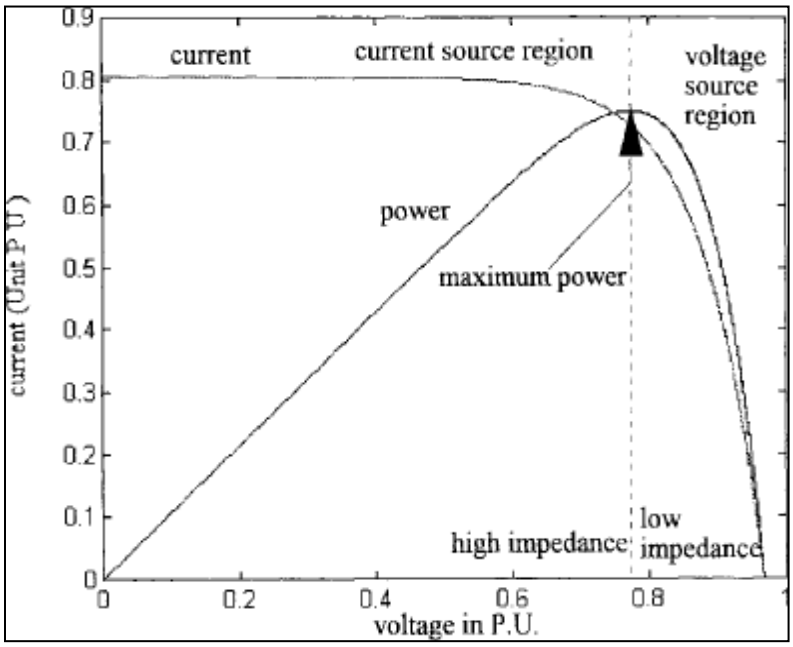

Figue III. 2: Solar array characteristic curves.

III. 4. Hill-climbing techniques

Both P&O and InCond algorithms are based on the "hill-climbing" principle, which consists of moving the operation point of the PV array in the direction in which power increases [19] and [22]. Hill-climbing techniques are the most popular MPPT methods due to their ease of implementation and good performance when the irradiation is constant [22]. The advantages of both methods are the simplicity and low computational power they need. The shortcomings are also well-known: oscillations around the MPP and they can get lost and track the MPP in the wrong direction during rapidly changing atmospheric conditions [23], [24]-[25]. These drawbacks will be explained later.

III.4.1 Perturb and observe

The P&O algorithm is also called "hill-climbing", but both names refer to the same algorithm depending on how it is implemented. Hill-climbing involves a perturbation on the duty cycle of the power converter and P&O a perturbation in the operating voltage of the DC link between the PV array and the power converter [27]. In the case of the Hill-climbing, perturbing the duty cycle of the power converter implies modifying the voltage of the DC link between the PV array and the power converter, so both names refer to the same technique.

In this method, the sign of the last perturbation and the sign of the last increment in the power are used to decide what the next perturbation should be. As can be seen in Figue 3, on the left

of the MPP incrementing the voltage increases the power whereas on the right decrementing the voltage increases the power.

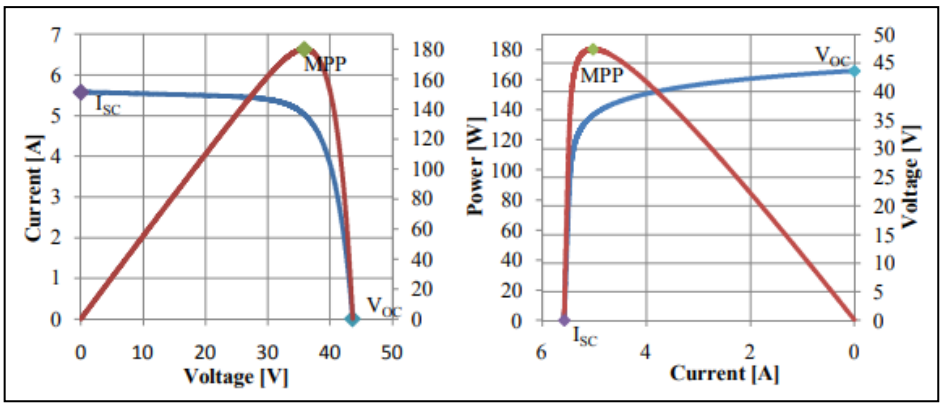

Figue III. 3: PV panel characteristic curves.

direction and if the power decreases, then the next perturbation should be in the opposite direction. Based on these facts, the algorithm is implemented [26]. The process is repeated until the MPP is reached. Then the operating point oscillates around the MPP. This problem is common also to the InCond method, as was mention earlier. A scheme of the algorithm is shown in Figue |III.3.

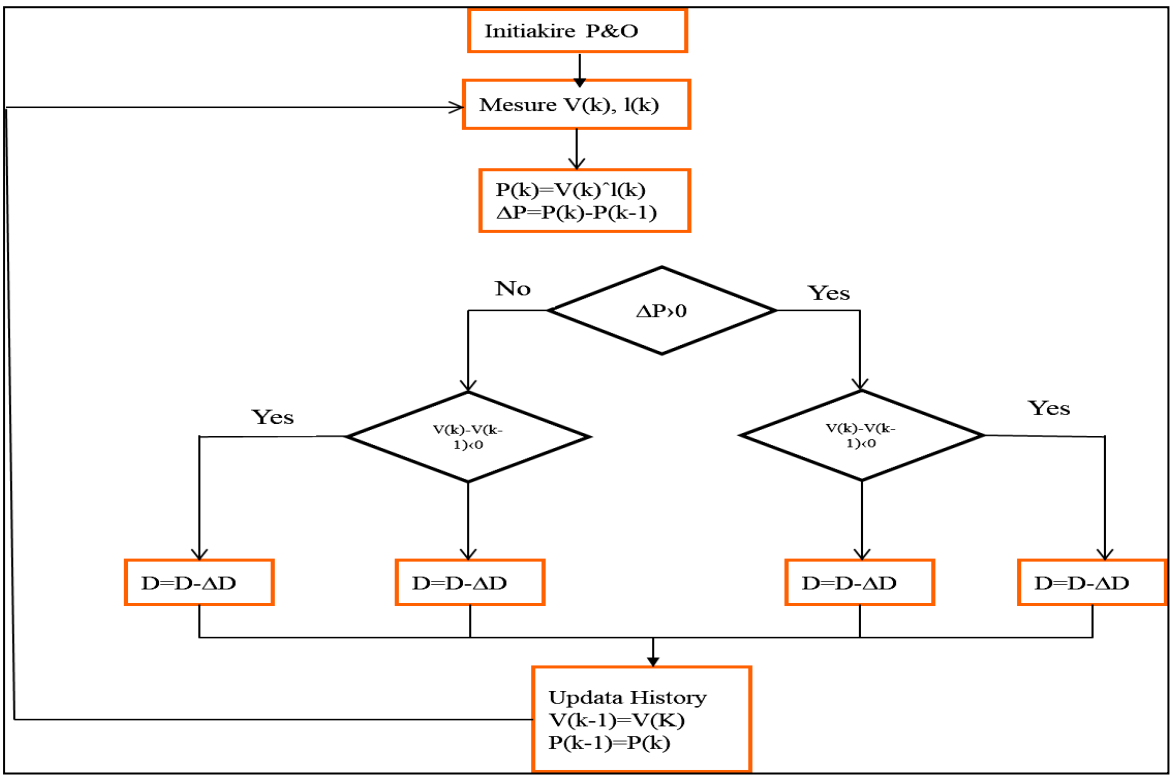

Figue III. 4: Flowchart of perturb and observe algorithm.

III.4.2 Incremental conductance (IC) method

The incremental conductance method uses the slope of the output power, and the voltage of the solar array is equal to zero at the maximum power point. The slope is positive on the left of MPP, negative on the right side of MPP, and it can be seen in Figue III.4:

- $\frac{dP}{dV} = 0, at\ MPP$ .....(III.1)
- $\frac{dP}{dV} > 0, left\ of\ MPP$ .....(III.2)
- $\frac{dP}{dV} < 0, right\ of\ MPP$..... ..(III.3)

According to the above explanation, it can be written followed,

- $\frac{dP}{dV} = \frac{d(VI)}{dV} = I + V\frac{dI}{dV} \cong I + V\frac{\Delta I}{\Delta V}$ .....(III.4)

(III.1), (III.2), (III.3) can be rewritten as:

- $\frac{dI}{dV} = -\frac{I}{V} I + $, $at\ MPP$ .....(III.5)
- $\frac{dI}{dV} > -\frac{I}{V}$, $left\ of\ MPP$ .....(III.6)
- $\frac{dPI}{dV} < -\frac{I}{V}$, $right\ of\ MPP$.....(III.7)

The flowchart of the IC method can be seen in Figue III.4

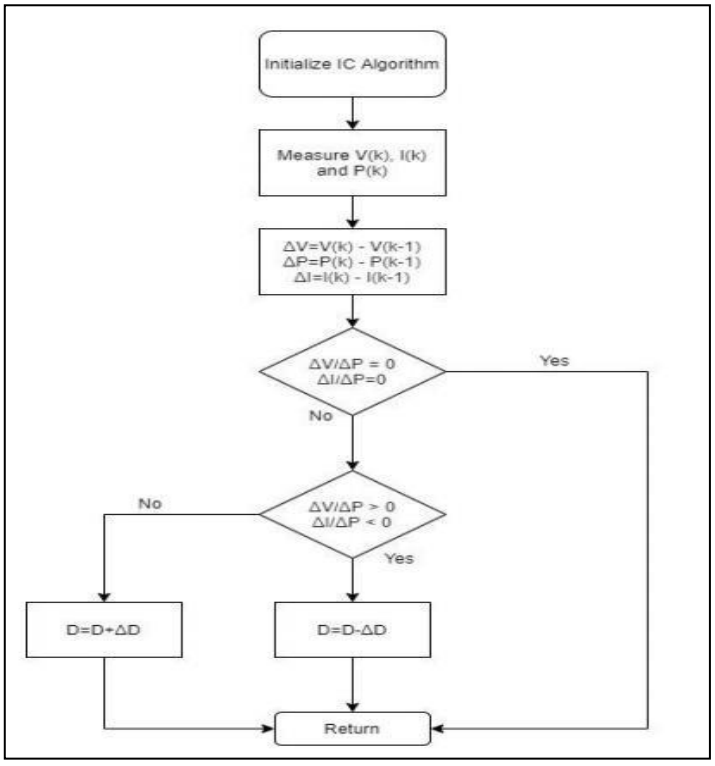

Figue III. 5: Flowchart of incremental conductance algorithm.

In both P&O and InCond schemes, how fast the MPP is reached depends on the size of the increment of ΔD.

The drawbacks of these techniques are mainly two. The first and main one is that they can easily lose track of the MPP if the irradiation changes rapidly [23], [24]-[27]. In case of step changes they track the MPP very well, because the change is instantaneous and the curve does not keep on changing. However, when the irradiation changes following a slope, the curve in which the algorithms are based changes continuously with the irradiation, as can be seen in Figue III.5, so the changes in the voltage and current are not only due to the perturbation of the voltage. As a consequence it is not possible for the algorithms to determine whether the change in the power is due to its own voltage increment or due to the change in the irradiation.

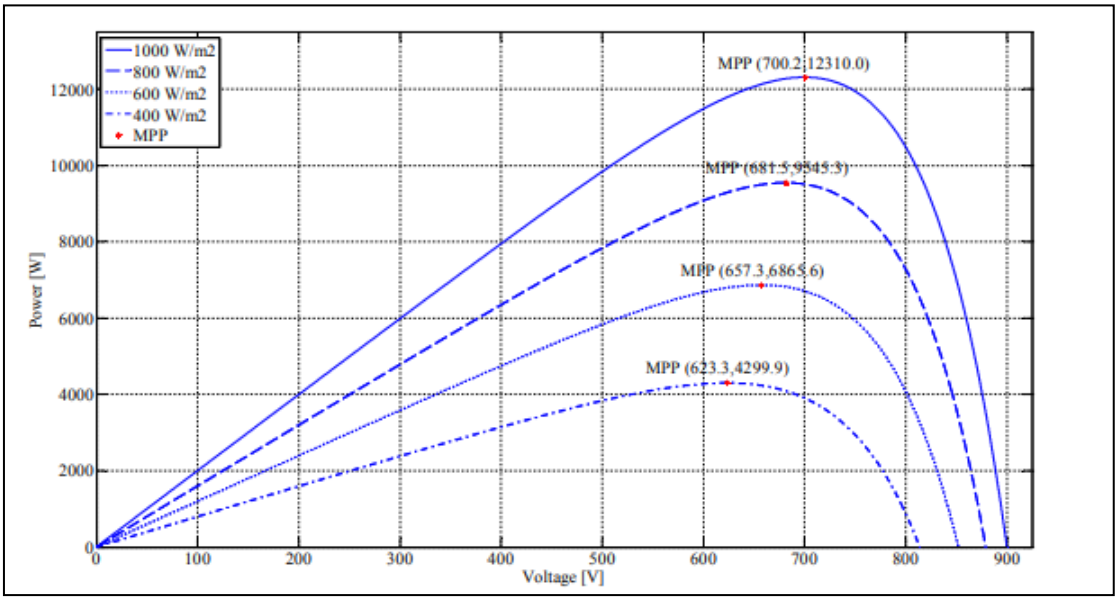

Figue III. 6: P-V curve depending on the irradiation.

The other handicap of both methods is the oscillations of the voltage and current around the MPP in the steady state [23], [28], [29] and [25]. This is due to the fact that the control is discrete and the voltage and current are not constantly at the MPP but oscillating around it. The size of the oscillations depends on the size of the rate of change of the reference voltage. The greater it is, the higher is the amplitude of the oscillations. However, how fast the MPP is reached also depends on this rate of change and this dependence is inversely proportional to the size of the voltage increments. The traditional solution is a trade off: if the increment is small so that the oscillations decrease, then the MPP is reached slowly and vice versa, so a compromise solution has to be found.

To overcome these drawbacks some solutions have been published in recent years. Regarding the rapid change of the irradiation conditions, Sera et al. published in [22] and [30] an improved P&O method, called "dP-P&O", in which an additional measurement is performed without perturbation in the voltage and current. In this way, every three consecutive samples the effect of the perturbation in the voltage (current) and the effect of the change in the atmospheric conditions can be evaluated so that the increment in the power used in the algorithm only contains the effect caused purely by the MPPT algorithm. Then the correct decision about the direction of the next perturbation can be taken. The efficiency of the tracking is improved. Although the method was tested using irradiation slopes, they were not the ones proposed in the new European Standard EN 50530 [29].

A different solution is suggested in [25], which considers the traditional P&O algorithm, in which the perturbation amplitude is tuned constantly taking into account the previous changes in the power. It also includes a stage in which the latest increment in the power is compared with the latest perturbation amplitude to determine if the power increment was due to a change in the irradiation. If this is the case, then the voltage perturbation is set to the same direction as the change in the power condition. The steady state error and the tracking speed are improved, but the algorithm has only been tested with irradiation step changes and not with the irradiation slopes proposed in [29].

In relationship with the oscillations around the MPP in steady state, Zhang et al. proposed in [29] a variable perturbation step for the P&O algorithm to reduce the oscillation around it. This modified P&O method determines also if the operating point is near to or far from the MPP and adjusts the size of the perturbation according to that: if the operating point is near to the MPP, the perturbation size is reduced and if the point is far, then it is increased. This technique improves the convergence speed and reduces the oscillation around the MPP. A similar technique is found in [29]: a variation of the traditional P&O algorithm in which the amplitude of the voltage perturbation is adapted to the actual operating conditions: large perturbation amplitudes are chosen far from the maximum whereas small ones are used near the MPP. The proposed algorithm requires initial panel identification and has to be tuned for each plant. With this technique the dynamic response and the steady state stability are improved. Unfortunately, the last two algorithms do not improve the tracking under changing irradiance conditions. Although the authors claim the performance is better, the algorithms have only been tested with irradiation step changes but not with irradiation ramps as proposed in the European Standard mentioned above [30].

A different solution is suggested in [23], which considers the traditional P&O algorithm, in which the perturbation amplitude is tuned constantly taking into account the previous changes in the power. It also includes a stage in which the latest increment in the power is compared with the latest perturbation amplitude to determine if the power increment was due to a change in the irradiation. If this is the case, then the voltage perturbation is set to the same direction as the change in the power condition. The steady state error and the tracking speed are improved, but the algorithm has only been tested with irradiation step changes and not with the irradiation slopes proposed in [30].

In relationship with the oscillations around the MPP in steady state, Zhang et al. proposed in [29] a variable perturbation step for the P&O algorithm to reduce the oscillation around it. This modified P&O method determines also if the operating point is near to or far from the MPP and adjusts the size of the perturbation according to that: if the operating point is near to the MPP, the perturbation size is reduced and if the point is far, then it is increased. This technique improves the convergence speed and reduces the oscillation around the MPP. A similar technique is found in [29]: a variation of the traditional P&O algorithm in which the amplitude of the voltage perturbation is adapted to the actual operating conditions: large perturbation amplitudes are chosen far from the maximum whereas small ones are used near the MPP. The proposed algorithm requires initial panel identification and has to be tuned for each plant. With this technique the dynamic response and the steady state stability are improved. Unfortunately, the last two algorithms do not improve the tracking under changing irradiance conditions. Although the authors claim the performance is better, the algorithms have only been tested with irradiation step changes but not with irradiation ramps as proposed in the European Standard mentioned above [30].

Many papers have been published about optimizing the parameters of these algorithms for different hardware configurations. In [23] the sample frequency for P&O is optimized and in [28] it is shown how the P&O MPPT parameters must be customized to the dynamic behaviour of the specific converter adopted. It has been traditionally said that the performance of InCond algorithm is better than the P&O. However, according to [23] and [28] the performance is similar if the parameters of the P&O method are optimized. In any case, both algorithms are based on the same principle and have the same problem so they have been analyzed together.

III.5. Fuzzy logic control:

The use of fuzzy logic control has become popular over the last decade because it can deal with imprecise inputs, does not need an accurate mathematical model and can handle nonlinearity. Microcontrollers have also helped in the popularization of fuzzy logic control [26].

The fuzzy logic consists of three stages: fuzzification, inference system and defuzzification. Fuzzification comprises the process of transforming numerical crisp inputs into linguistic variables based on the degree of membership to certain sets. Membership functions, like the ones in Figue III. 7, are used to associate a grade to each linguistic term. The number of membership functions used depends on the accuracy of the controller, but it usually varies between 5 and 7 [26], [32]-[31]. In Figue III.7 seven fuzzy levels are used: NB (Negative Big), NM (Negative Medium), NS (Negative Small), ZE (Zero), PS (Positive Small), PM (Positive Medium) and PB (Positive Big). The values a, b and c are based on the range values of the numerical variable. In some cases the membership functions are chosen less symmetric or even optimized for the application for better accuracy [26], [32].

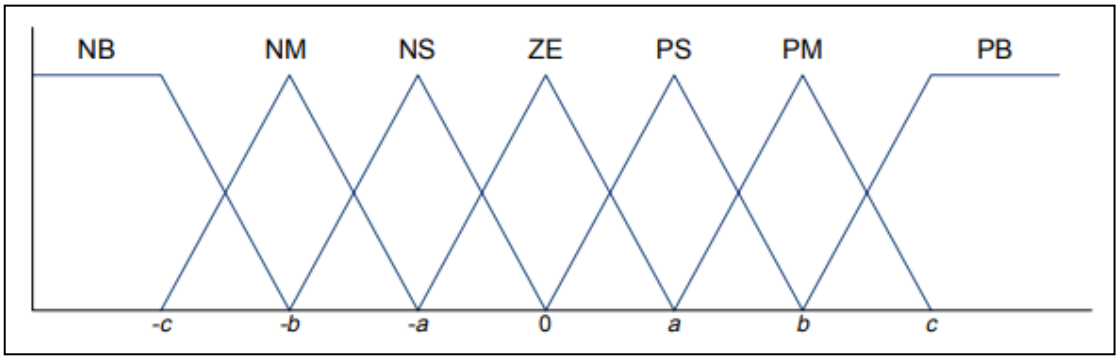

Figue III. 7: Membership functions.

The inputs of the fuzzy controller are usually an error, E, and the change in the error, ΔE. The error can be chosen by the designer, but usually it is chosen as $\Delta P/\Delta V$ because it is zero at the MPP. Then E and ΔE are defined as follows:

$$E=\frac{P(K)-P(K-1)}{V(K)-V(K-1)} \quad \text{(III.8)}$$

$$\Delta E=(k)-E(k-1) \quad \text{(III.9)}$$

In other cases $\Delta P \Delta I/$ is used as error [32] or other inputs are considered, as in [28], where ΔU and ΔP are used.

The output of the fuzzy logic converter is usually a change in the duty ratio of the power converter, ΔD, or a change in the reference voltage of the DC-link, ΔV. The rule base, also known as rule base lookup table or fuzzy rule algorithm, associates the fuzzy output to the fuzzy inputs based on the power converter used and on the knowledge of the user. Table I shows the rules for a three phase inverter, where the inputs are E and ΔE, as defined in (7) and (8), and the output is a change in the DC-link voltage, ΔV. For example, if the operating point is far to the right of the MPP, E is NB, and ΔE is zero, then to reach the MPP the reference voltage should decrease, so ΔE should be NB (Negative) to move the operating point towards the MPP.

E\dE	**NB**	**NM**	**NS**	**ZE**	**PS**	**PM**	**PB**
NB	NB	NB	NB	NB	NM	NS	ZE
NM	NB	NB	NB	NM	NS	ZE	PS
NS	NB	NB	NM	NS	ZE	PS	PM
ZE	NB	NM	NS	ZE	PS	PM	PB
PS	NM	NS	ZE	PS	PM	PB	PB
PM	NS	ZE	PS	PM	PB	PB	PB
PB	ZE	PS	PM	PB	PB	PB	PB

Table III: Rules Base table.

The last stage of the fuzzy logic control is the defuzzification. In this stage the output is converted from a linguistic variable to a numerical crisp one again using membership functions as those in Figue III. 8. There are different methods to transform the linguistic variables into crisp values. It can be said that the most popular is the center of gravity method. However the analysis of these methods is beyond the scope of this thesis.

The advantages of these controllers, besides dealing with imprecise inputs, not needing an accurate mathematical model and handling nonlinearity, are fast convergence and minimal oscillations around the MPP. Furthermore, they have been shown to perform well under step changes in the irradiation. However, no evidence was found that they perform well under irradiation ramps. Therefore, their performance under the conditions specified in [31] for testing the dynamic MPPT efficiency is unknown. Another disadvantage is that their effectiveness depends a lot on the skills of the designer; not only on choosing the right error computation, but also in coming up with an appropriate rule base [26].

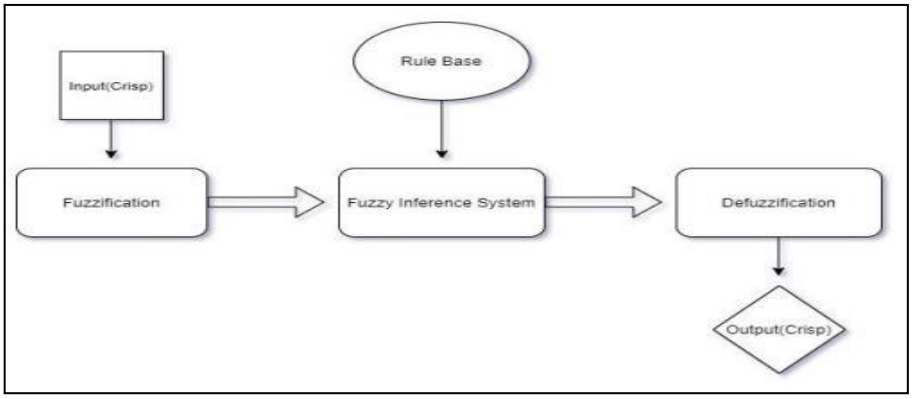

Figue III.8: Flowchart of the fuzzy logic control.

III.6. Neural networks:

Another MPPT method well adapted to microcontrollers is Neural Networks [26]. They came along with Fuzzy Logic and both are part of the so called "Soft Computing". The simplest example of a Neural Network (NN) has three layers called the input layer, hidden layer and output layer, as shown in Figue III. 9. More complicated NN's are built adding more hidden layers. The number of layers and the number of nodes in each layer as well as the function used in each layer vary and depend on the user knowledge. The input variables can be parameters of the PV array such as VOC and ISC, atmospheric data as irradiation and temperature or a combination of these. The output is usually one or more reference signals like the duty cycle or the DC-link reference voltage.

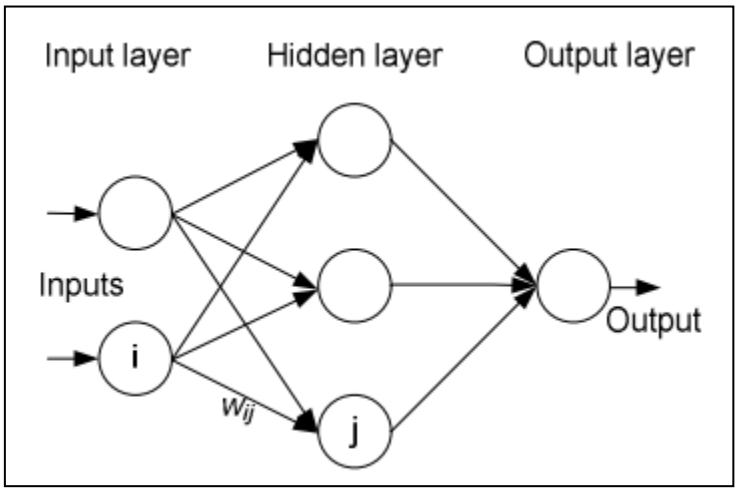

Figue III. 9: Neural network.

The performance of the NN depends on the functions used by the hidden layer and how well the neural network has been trained. The links between the nodes are all weighted. In Figue 9 the weight between the nodes i and j is labelled as wij. The weights are adjusted in the training process. To execute this training process, data of the patterns between inputs and outputs of the neural network are recorded over a lengthy period of time, so that the MPP can be tracked accurately.

The main disadvantage of this MPPT technique is the fact that the data needed for the training process has to be specifically acquired for every PV array and location, as the characteristics of the PV array vary depending on the model and the atmospheric conditions depend on the location. These characteristics also change with time, so the neural network has to be periodically trained.

CHAPTER VI

Simulation and Realization of the system

VI.1. Introduction

Simulation is a tool for evaluating the theoretical performance of a system. Indeed this part will allow us to carry out simulations of a photovoltaic generator followed by a DC/DC converter and to test the MPPT commands. This allows us to modify the system parameters easily such as the metrological conditions, and to visualize the contribution of the command on the photovoltaic generator. MATLAB software and its associated graphical extension SIMULINK are part of a set of tools integrated into signal processing, present the possibility of simulating systems at their continuous and discrete states, so it is well suited for testing digital MPPT commands. This chapter is devoted to the simulation and the comparative study between control methods in order to obtain better results.

VI.2. Simulation of a photovoltaic system

As we showed in the previous chapter, for the photovoltaic (PV) generator to operate under optimal conditions, it must be equipped with an adaptation quadripole. maximum power (PPM) of the PV generator and this when the system is placed in an environment where the meteorological conditions (sunshine, temperature) and load are stable.

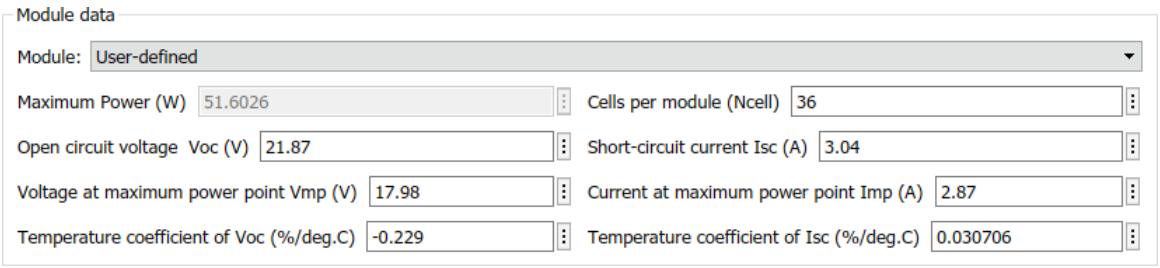

Figue VI.1: Data on the electrical characteristics of the PV module taken from Mat-lab/Simulink.

buck-boost converter	Values
Input capacitance (Cin)	100 µF
Inductance (L)	0.018mH
Capacitance (C)	100 µF
Load resistance (R)	30 W

Table VI.1 : Buck-Boost converter parameter.

VI.2.1 Matlab/Simulink diagram of photovoltaic system

a) PandO mode in stable radiation

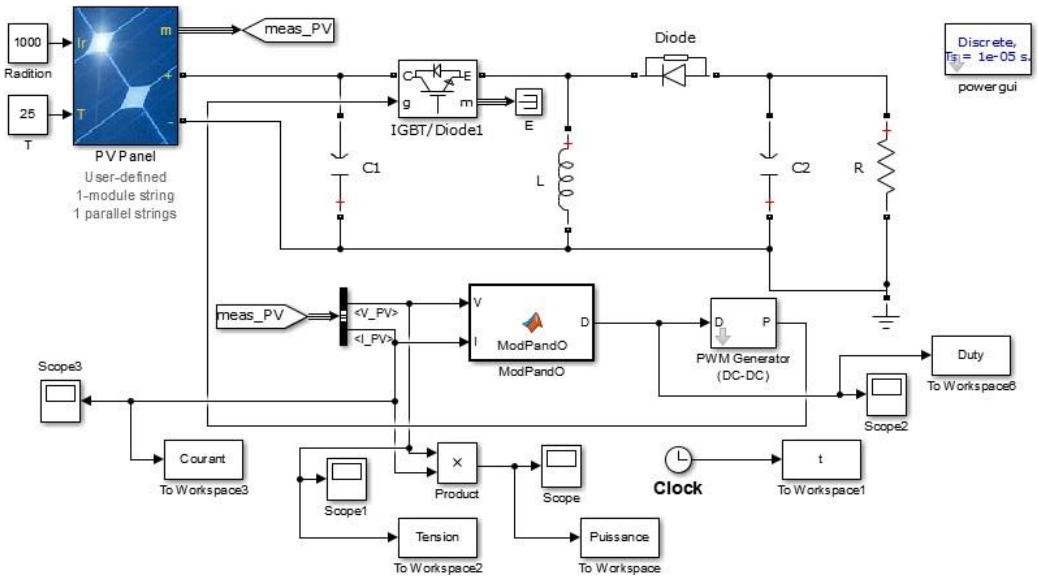

Figue VI.2 : Matlab/Simulink diagram of PV system with stable radiation.

b) PandO mode in variable radiation

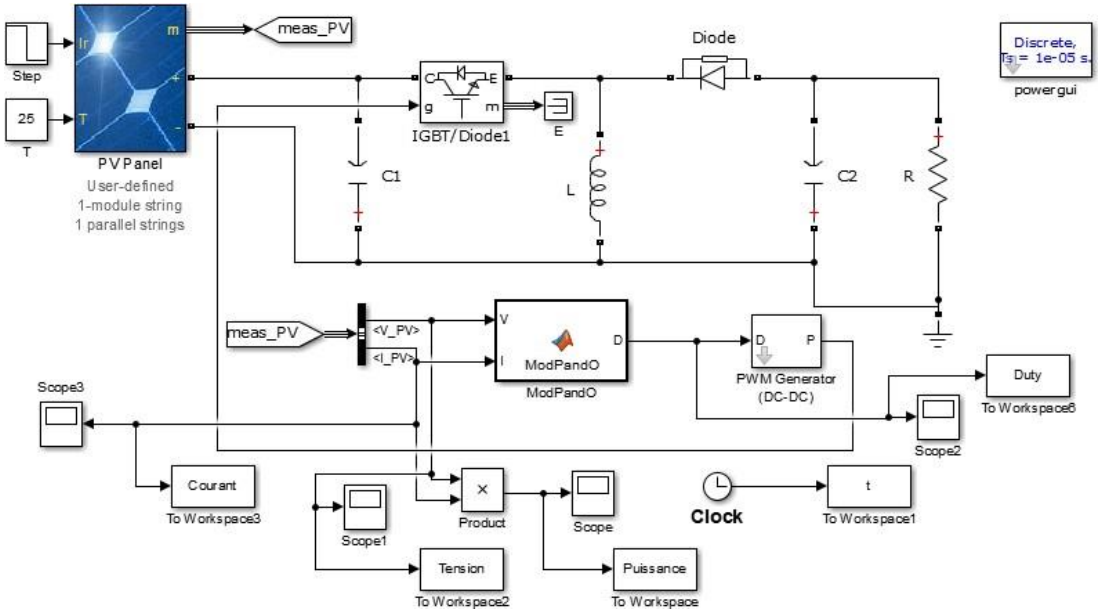

Figue VI .3 : Matlab/Simulink diagram of PV system with variable radiation.

c) Cuckoo search method

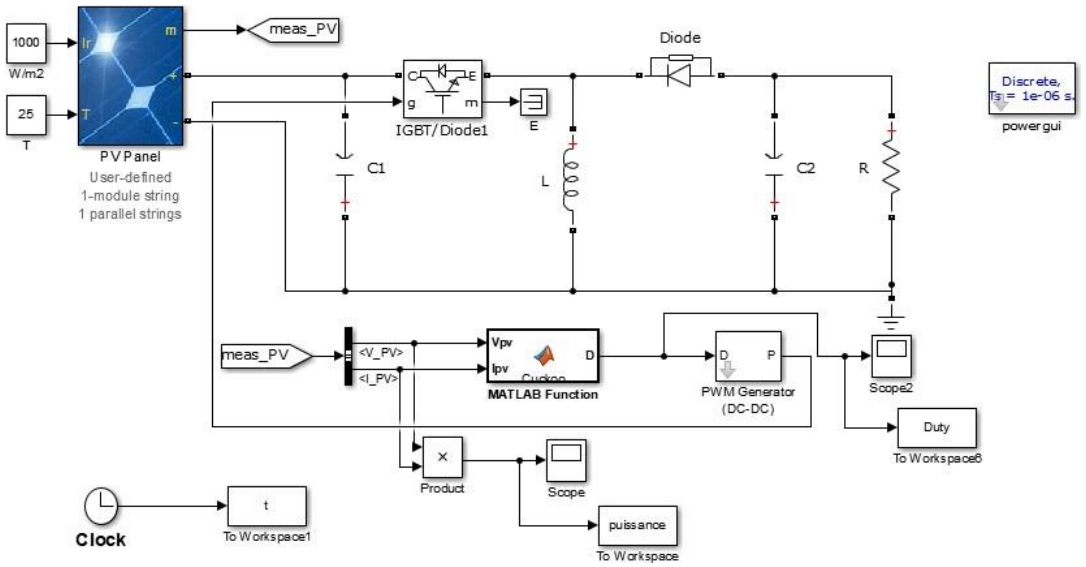

Figue VI.4 : Matlab/Simulink diagram of PV system (CS).

VI.2.2 Simulation results:

a) PO algorithm (stable radiation):

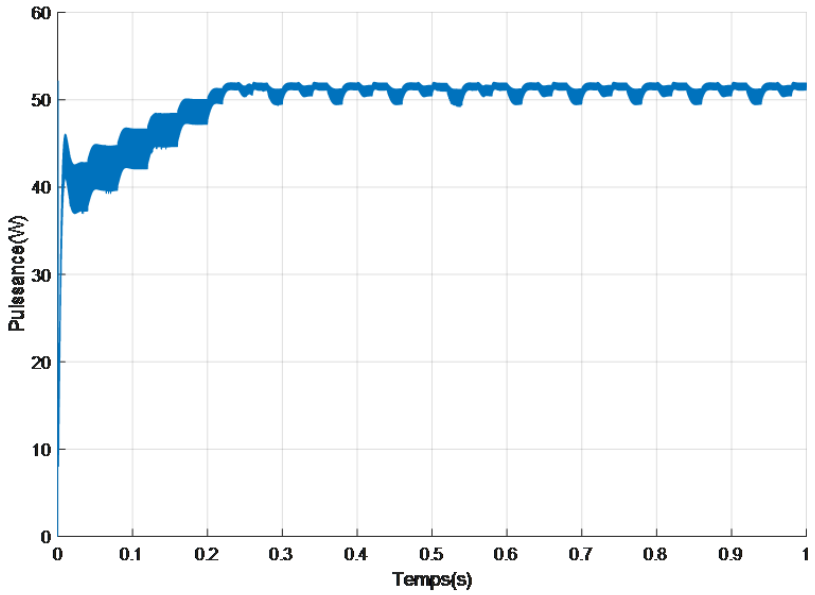

Figue VI.5 : Power PV simulation result

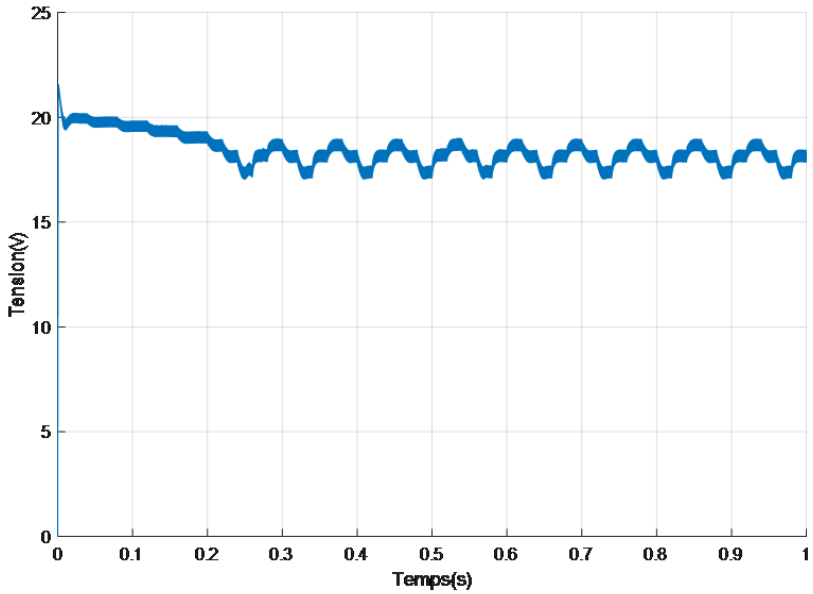

Figue VI.6 : PV voltage simulation result

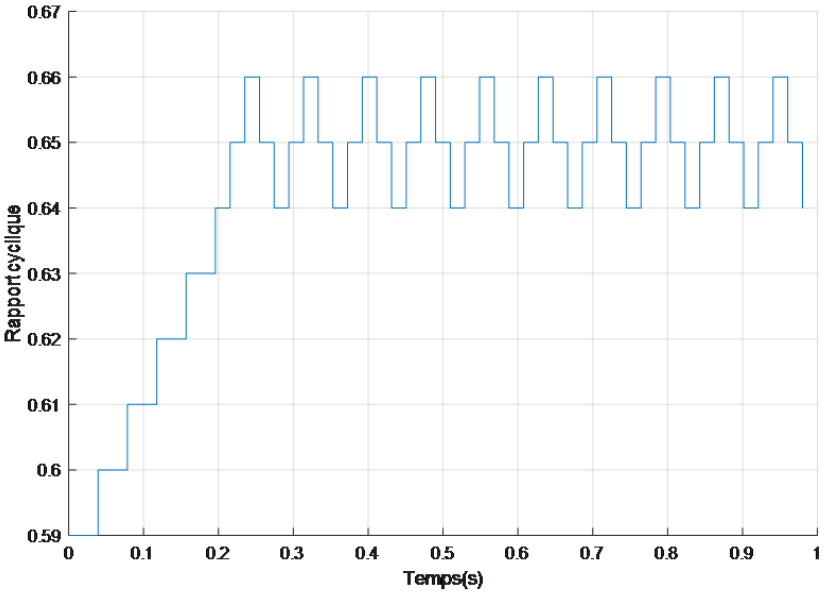

Figue VI.7 : Changement de rapport ciclique à l'aide l'algorithme suivi par le carte d'arduino.

b) PO algorithm (radiation variable)

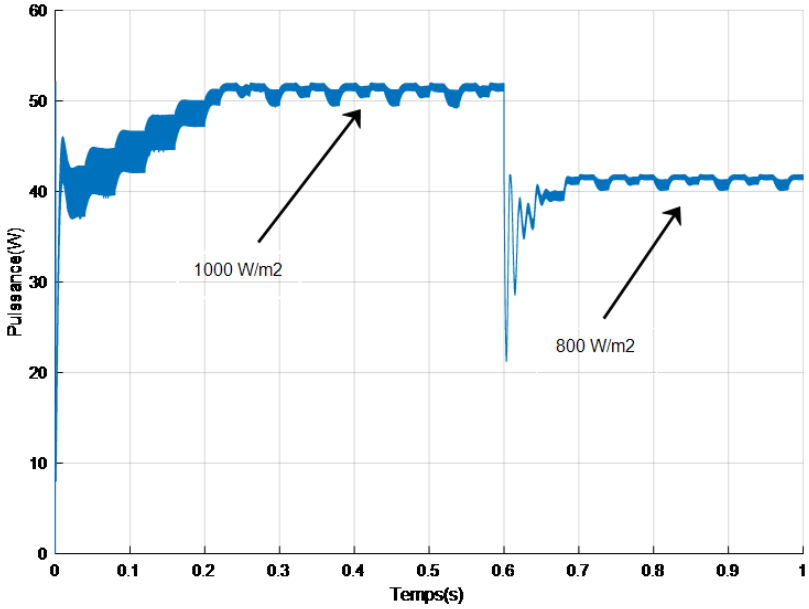

Figue VI .8 : Power PV simulation result

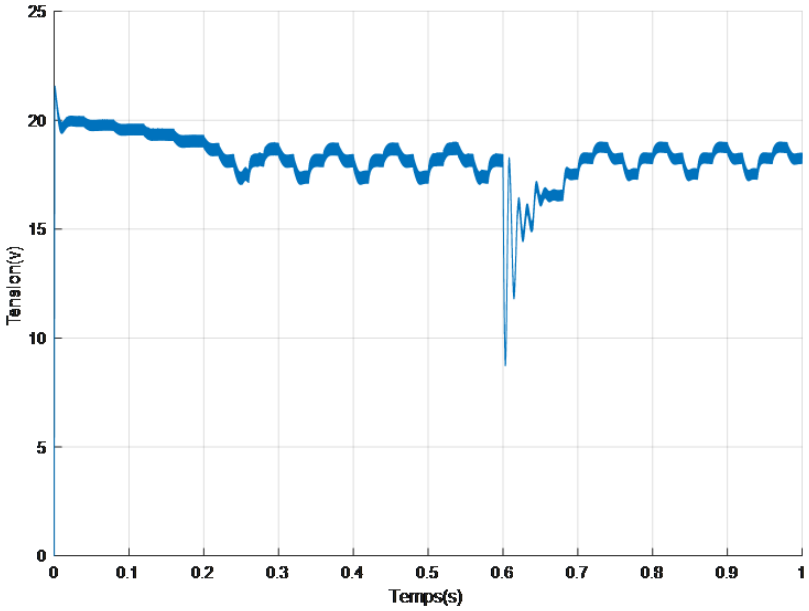

Figue VI.9 : PV voltage simulation result**.**

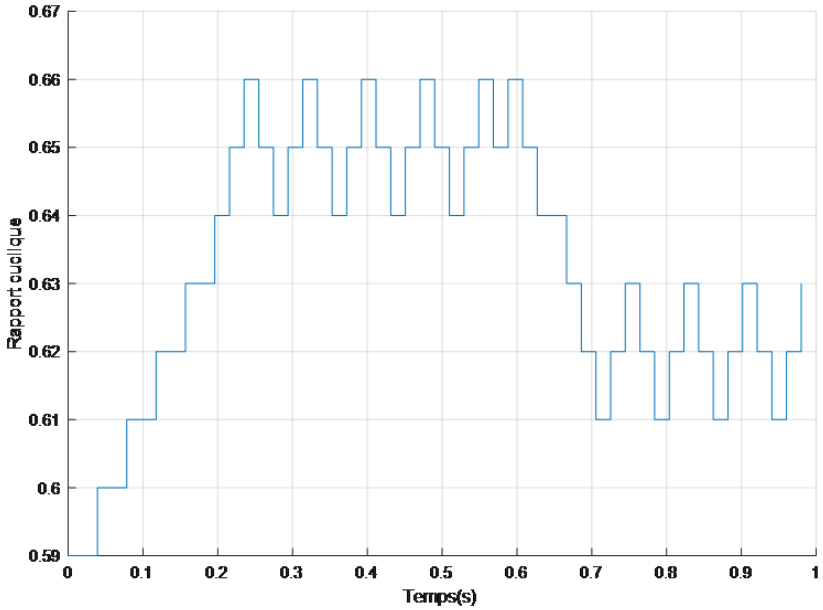

Figue VI .10: Cyclic gear change using
the algorithm followed by the arduino board.

c) Cuckoo search algorithm

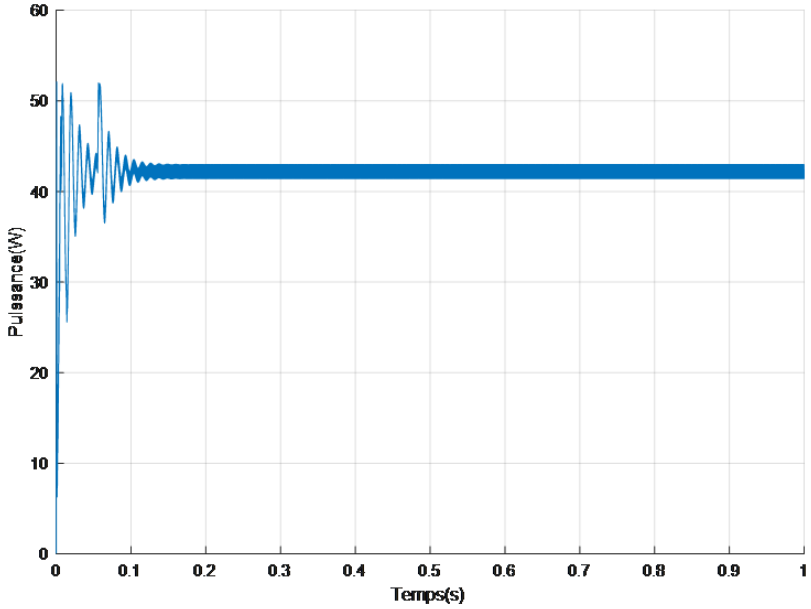

Figue **VI**.11 : Power PV simulation result

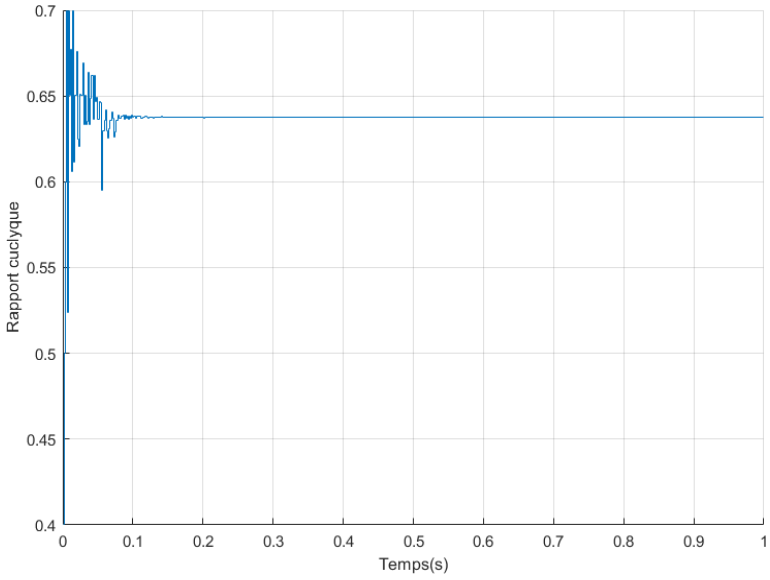

Figue VI.12: Cyclic gear change using
the algorithm followed by the arduino board.

e) Simulation results of MPP tracking waveforms

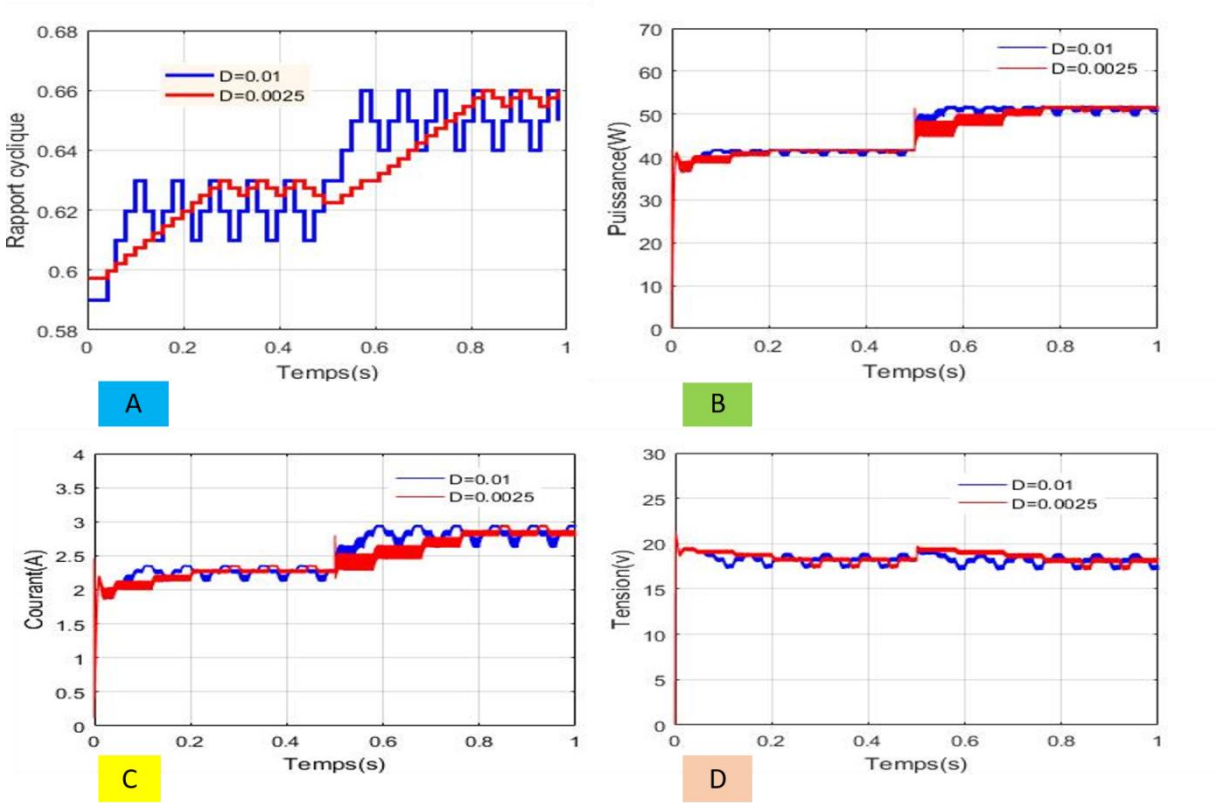

FigureVI. : Simulation results of MPP tracking waveforms: (A) duty cycle, (B) PV power, (C) PV current and (D) PV voltage for steady state operation with two setting factors MPPT scale: (blue) PO based on 0.01 and (red) PO based on 0.0025.

VI.3. Material used

VI.3.1 The microcontroller

•Definition

In this regard, the ArduinoMega is similar to the Due in that it has 54 I/O pins. However, instead of being powered by an ARM processor, it is powered by an ATmega2560.

The processor runs at 16 MHz and has 256 kilobytes of ROM, 8 kilobytes of RAM, 4 kilobytes of EEPROM and operates at 5 volts, making it compatible with most consumer electronics.

The ArduinoMega has 16 analog inputs, 15 PWM outputs, pinout similar to Due, and hardware compatible with Arduino shields. Software compatibility with Mega, as with Due, cannot always be guaranteed.

Figue VI .13 : Arduino MEGA2560.

Category	Value
Microcontroller	Atmega 2560
Clock frequency	16MHZ
Operating voltage	5V
Input voltage (recommended)	7-12V
Input voltage (limits)	6-20V
Digital doors	54 inputs and output
Analog gates	16 analog inputs
Max current per I/O pin	40mA
Max current per pin3.3V	50mA
Memory	256 KB flash, 8 KB SRAM, 4 KB
Bootloader	EEPROM
Interface	8 KB (in flash memory)
Dimensions	USB
Price	10.16cm*5.3cm
	$47

Table VI.2 : the arduino MEGA board**.**

VI.3.2 The solar panel

We used the 21.87V, 50W laboratory benchtop solar panel shown in Figue (VI.14).

Figue VI .14 : Photo real PV panel.

PV panel nameplate

Figue VI.15 : PV panel nameplate

.

VI.3.3 Buck-Boost Converter

✓ The Buck-Boost converter is composed of

- two capacitor Cin=3000µf, Cout=3000µf, connected to the terminals of the module to filter the chopper input voltage and reduce input and output ripples.
- An inductor: L=0.018mH.
- An IRF830 MOSFET.

Figue VI.16: Real photo of Buck-Boost converter board.

VI.3.4 Buck-Bosst converter control circuit

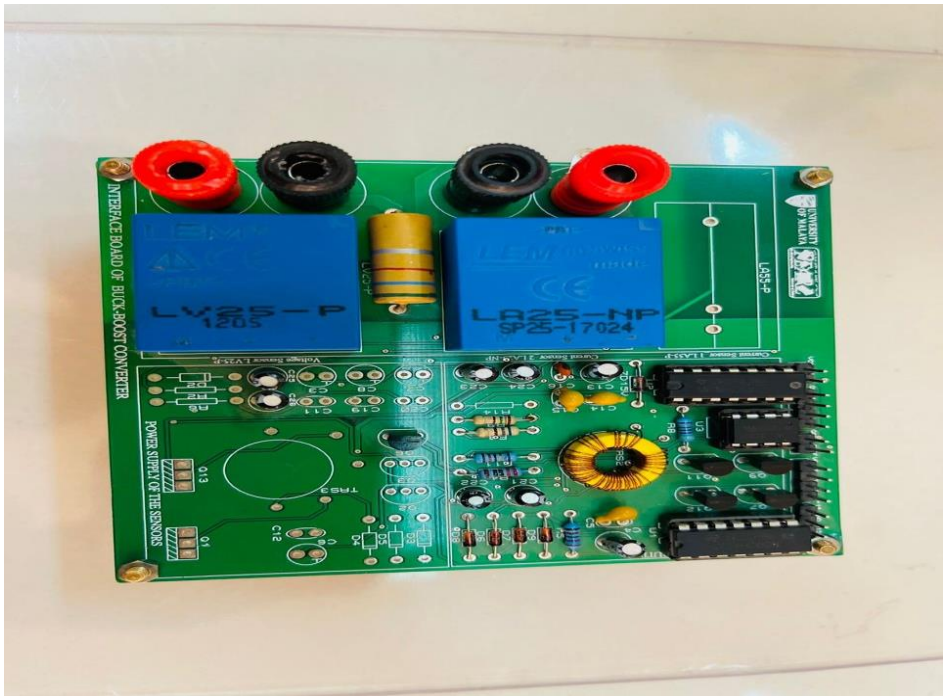

Figue VI.17: Real photo of Buck-Boost converter

VI.4. Realization of the system

In this part, an efficient arduino/matlab based maximum power point tracking system using a real photovoltaic panel is designed. We will present the experimental results of the experiment, working with PO and INC.

We did a real test measuring the cloudy day, the sunny day and the false shaded panel to assess the effectiveness of the proposed method in climatic conditions variables.

User does not need to do any programming in Arduino IDE. Everything will be done in Simulink using S-function builder. This solution consists on the one hand in using the functions offered by Simulink which makes it possible to send and acquire data via the serial port (USB) and on the other hand to process and visualize this data in real time.

Also we needed to make the arduino PWM output reach 20kHz at least because arduino using special function code S.

1- Hardware input, where Vpv and Ipv sensors will be read using arduino,

2- Data processing by MPPT algorithms and transfer the control signal (PWM) to the Boost converter.

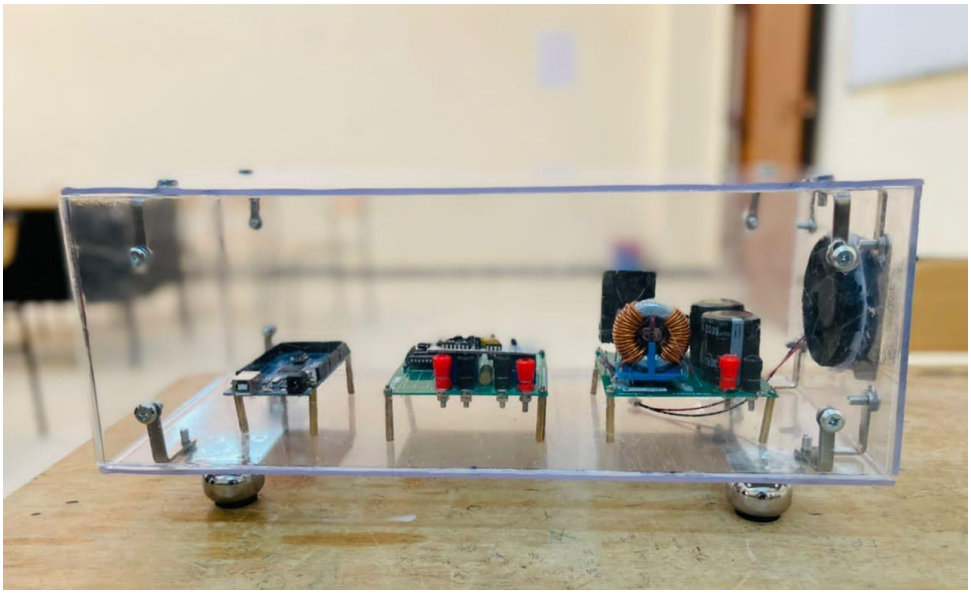

Figue **VI**.18 : Real photo of control part of our system

Figue **VI**.19 :Real photo of PV system.

VI.4.1 Practical results

a) Sunny day

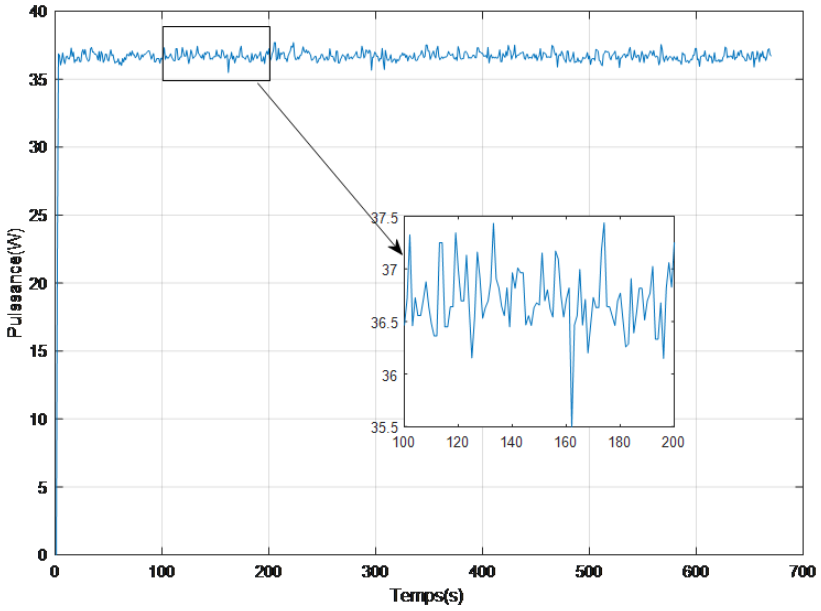

Figue VI.20: Practical result of the PO algorithm.

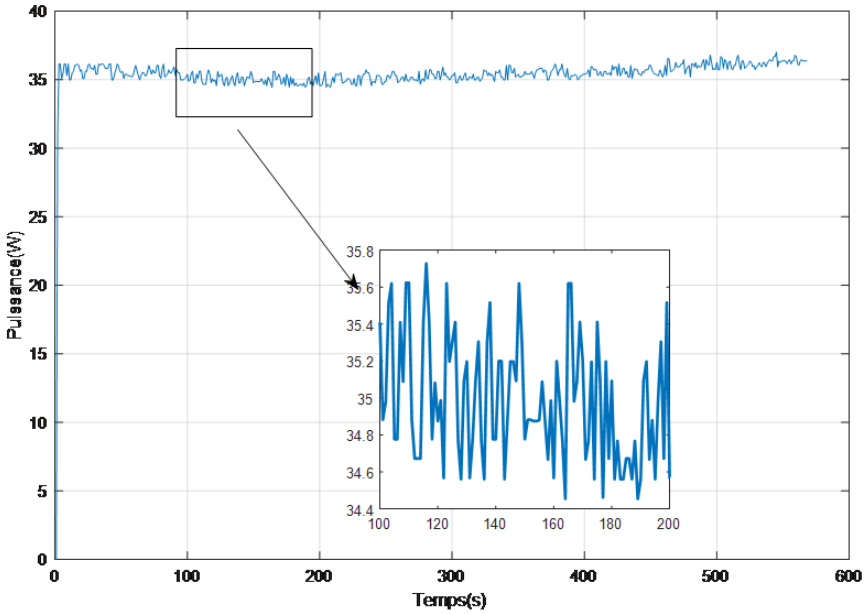

Figue VI.21 : Practical result of the INC algorithm

b) Cloudy day

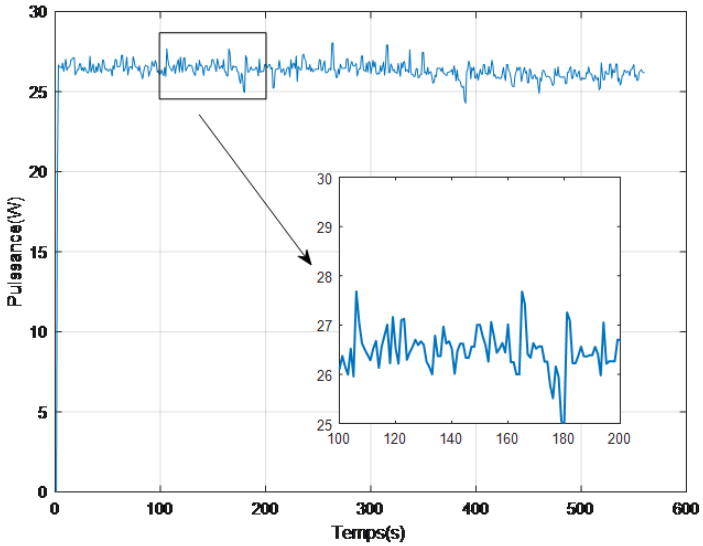

Figue VI.22: Practical result of the PO algorithm.

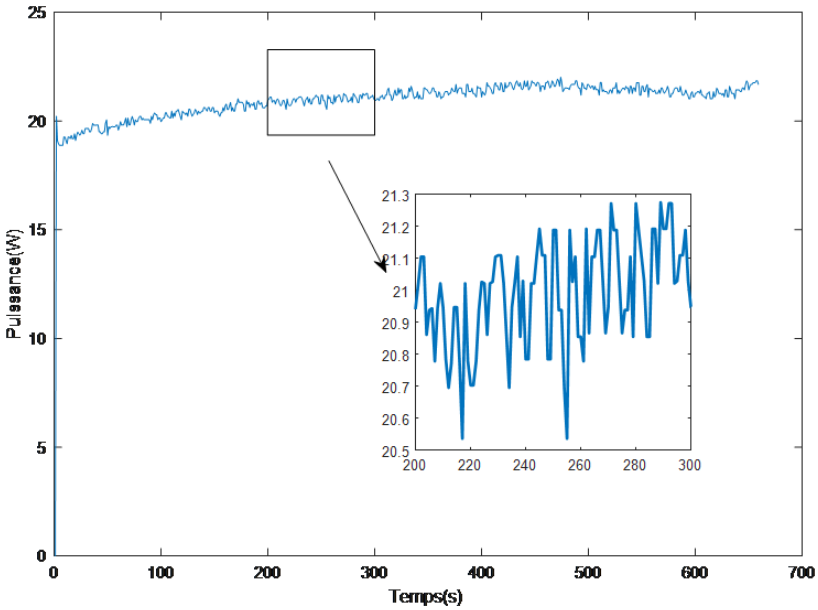

Figue VI.23 :Practical result of the INC algorithm.

c) Shaded Pane

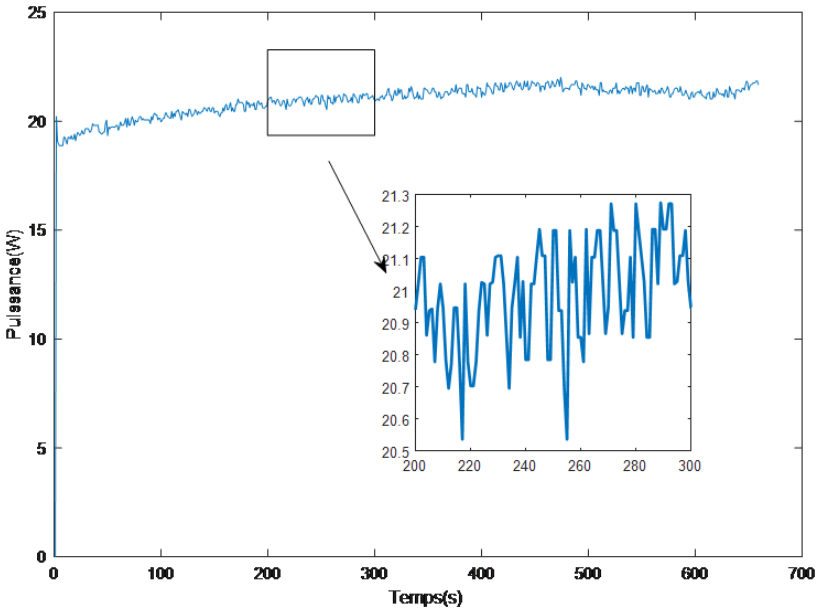

Figue VI.24 : Practical result of the INC algorithm.

d) PWM signal transferred from control to converter

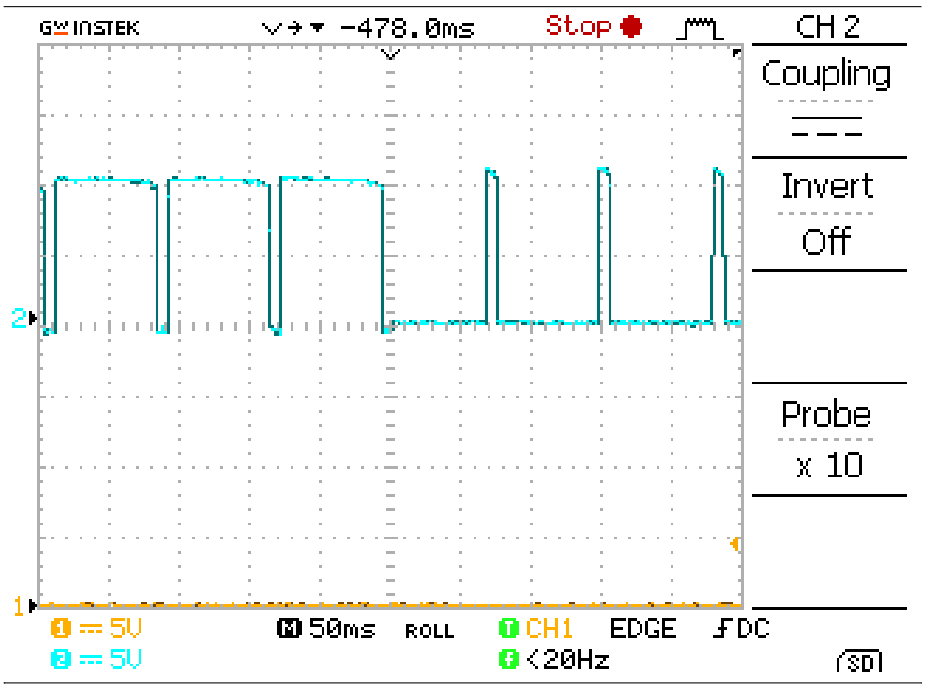

F**igue VI**.25: PWM signal

e) Output voltage change by PWM constant control [0.9;0.1]

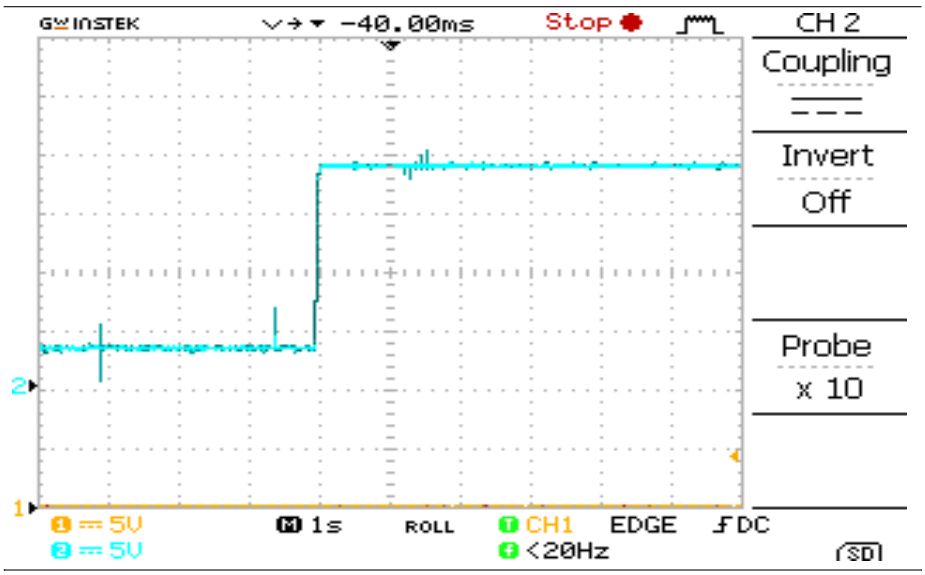

Figue VI.26 : Output voltage change by PWM constant control [0.9;0.1].

VI.5.Conclusion

This chapter is devoted to the installation and simulation under matlab/simulink of a PV system, we have controlled the system by different types of MPPT algorithms, it can be concluded that with the proposed MPPT algorithms, the PV panel can deliver the maximum power as shown in the experimental results both PO and INC has close results. However, it has the ability to reduce the disturbed voltage when the MPP was recognized. This action directly preserves a more stable output power compared to conventional MPPT where the output power fluctuates around MPP.

As per the analysis of our method, has a large key space and high level security. Thus the analysis proves the safety and effectiveness.

CONCLUTION

CONCLUTION

The work presented in this thesis deals with the simulation, and implementation of a photovoltaic system operating with a BUCK- BOOST converter. This converter has the advantage of being a voltage booster which allows this system to adapt to changes in weather and to extract the maximum power available to the load. The simulation and experi mental results have demonstrated the interest of a device for researching maximum power. The algorithms, P&O , CS and INC are chosen to be implemented in an Arduino Mega2560 board, in order to track the operating point at maximum power of the PV panel. From the simulation and experimental results, it can be concluded that with the proposer algorithms, the PV panel can deliver the maximum power. However, Although we could not actually implement them and more accurate than that of the (P&O), INC and cuckoo search:CS , it has the ability to reduce the disturbed power when the MPP has been recognized.

BIBLIOGRAPHIE

[1]: Asia BOURABI. Élaboration et Caractérisation des Couches Minces CuInSe2 par Électrodéposition. Thèse de université MENTOURI - CONSTANTINE faculté des science exactes département de physique.2009.

[2] A. Attar, "Les énergies renouvelables" ancien PDG de Sonatrach et ancien Ministre des Ressources en Eau.

[3]: Energies Renouvelables. http://www.energies-renouvelables.org.

[4] Brahimi (MEM), "Situation des énergies renouvelables en Algérie". Conférence sur la maîtrise de l'énergie et de l'environnement dans un contexte d'économie de marche, 2001, Hôtel Sheraton, Alger, Algérie.

[5] Green, Martin A. *Solar Cells; Operating Principles, Technology, and System Applications* Prentice Hall Inc., 1982

[6] Antonio Luque and Steven Hegedus,"Handbook of Photovoltaic Science and Engineering", John Wiley & Sons Ltd, 2003

[7]: MEFLAH AISSA. Modulation et commande d'une chaine de pompage photovoltaïque. ECOLE DOCTORALE « Energies Renouvelables » université ABOU BEKR BELKAID – TLEMCEN.2011.

[8] L. ABBASSEN ' Etude de la connexion au réseau électrique d'une centrale photovoltaïque' Mémoire de magister, université mouloud Mammeri Tizi ouzzo, 2011.

[9] S. PETIBON ' Nouvelles architectures distribuées de gestion et de conversion de l'énergie pour les applications photovoltaïques', université de Toulouse, 2009.

[10] S. Bellakehal, *«Conception & Commande des Machines à Aimants Permanents Dédiées aux Energies Renouvelables»,* thèse de Doctorat, Université de Constantine, Algérie, 2010.

[11] M. Adouane, *«Etude et conception d'une stratégie de commande d'un onduleur connecté au réseau électrique»,* Mémoire de magistère, Ecole Nationale Polytechnique, Alger, Algérie, 2008.

[12] M. Makhlouf, *«Etude et optimisation d'un modèle de conversion d'énergie photovoltaïque application au pompage»,* mémoire de magister, université Mentouri Constantine, Algérie, 2006.

[13]. N. Abouchabana, « Etude d'une nouvelle topologie buck-boost appliquée à un MPPT », *Mémoire de Magistère, Ecole Nationale Polytechnique, Alger,2009.*

[14]. https://fr.wikipedia.org.

[15]. M .Touaref , « Etude et simulation d'un convertisseur AC/DC type BUCK (Abaisseur de tension) », *thèse master en génie électrique université de Biskra, juin*

2014.

[16] Christian Blum, Daniel Merkle , « Swarm Intelligence: Introduction and Applications », Natural Computing Series, Springer-Verlag, Berlin Heidelberg, 2008**.**

[17] Mirjana Milosevic: "On the Control of Distributed Generation in Power System" thesis for the degree of Doctor of Technical Sciences, Swiss Federal Institute of Technology Zurich, 2007.

[18] Chihchiang Hua, *Member, IEEE,* Jongrong Lin, and Chihming Shen: "Implementation of a DSP-Controlled Photovoltaic System with Peak Power Tracking" IEEE TRANSACTIONS ON INDUSTRIAL ELECTRONICS, VOL. 45, NO. 1, FEBRUARY 1998.

[19] Mohammad A. S. Masoum, Hooman Dehbonei, and Ewald F. Fuchs, Fellow: "Theoretical and Experimental Analyses of Photovoltaic Systems with Voltage- and Current-Based Maximum Power-Point Tracking" IEEE TRANSACTIONS ON ENERGY CONVERSION, VOL. 17, NO. 4, DECEMBER 2002.

[20] D. Shmilovitz: "On the Control of Photovoltaic Maximum Power Point Tracker Via Output Parameters" IEE Proc.-Electr. Power Appl., Vol. 152, No. 2, March 2005.

[21] Vikrant.A.Chaudhari: "Automatic Peak Power Tracker for Solar PV Modules Using DSPACER Software" Thesis for the award of the Degree of Master of Technology in Energy, July 2005.

[22] N. Femia, G. Petrone, G. Spagnuolo, M. Vitelli, "Optimizing sampling rate of P&O MPPT technique," in Proc. IEEE PESC, 2004.

[23] T. Esram, P.L. Chapman, "Comparison of Photovoltaic Array Maximum Power Point Tracking Techniques," IEEE Transactions on Energy Conversion, vol. 22, no. 2, pp. 439- 449, June 2007.

[24] Overall efficiency of grid connected photovoltaic inverters, European Standard EN 50530, 2010.

[25] D. Sera, T. Kerekes, R. Teodorescu, F. Blaabjerg, "Improved MPPT Algorithms for Rapidly Changing Environmental Conditions," in Proc. 12th International Conference on Power Electronics and Motion Control, 2006, pp. 1614-1619.

[26] D. Sera, T. Kerekes, R. Teodorescu, F. Blaabjerg, "Improved MPPT method for rapidly changing environmental conditions," in Proc. IEEE International Symposium on Industrial Electronics, 2006, vol. 2..

[27] N. Femia, G. Petrone, G. Spagnuolo, M. Vitelli, "Optimization of perturb and observe maximum power point tracking method," IEEE Transactions on Power Electronics, vol. 20, no. 4, pp. 963-973, July 2005.

[28] K.H. Hussein, I. Muta, T. Hoshino, M. Osakada, "Maximum photovoltaic power tracking: an algorithm for rapidly changing atmospheric conditions," IEE Proceedings on Generation, Transmission and Distribution, vol. 142, no. 1, pp. 59-64, Jan 1995.

[29] C. Zhang, D. Zhao, J. Wang, G. Chen, "A modified MPPT method with variable perturbation step for photovoltaic system," in Power Electronics and Motion Control Conference, 2009.

[30] W. Xiao, W. G. Dunford, "A modified adaptive hill climbing MPPT method for photovoltaic power systems," in Proc. IEEE PESC, 2004..

[31] N. Patcharaprakiti, S. Premrudeepreechacharn, "Maximum power point tracking using adaptive fuzzy logic control for grid-connected photovoltaic system," in Proc. IEEE Power Engineering Society Winter Meeting, 2002.

[32] J. Li, H. Wang, "Maximum power point tracking of photovoltaic generation based on the fuzzy control method," in Proc. International Conference on Sustainable Power Generation and Supply, 2009.